Identification of pneumococcal proteins that are functionally linked to penicillin-binding protein 2b (PBP2b).

Daniel Straume, Gro Anita Stamsås, Kari Helene Berg, Zhian Salehian and Leiv Sigve Håvarstein*

Department of Chemistry, Biotechnology and Food Science, Norwegian University of Life Sciences, NO-1432 Ås, Norway.

Running title: Identification of PBP2b accessory proteins

Key words: *Streptococcus pneumoniae*, elongasome, PBP2b, MreD, DivIVA, RodA

* Corresponding author:

Leiv Sigve Håvarstein

Department of Chemistry, Biotechnology, and Food Science,

Norwegian University of Life Sciences, P.O. Box 5003, NO-1432 Ås, Norway.

Tlf: 47-67232493

Fax : 47-64965901

E-mail: sigve.havarstein@nmbu.no

Summary

The oval shape of pneumococci results from a combination of septal and lateral peptidoglycan synthesis. The septal cross-wall is synthesized by the divisome, while the elongasome drives cell elongation by inserting new peptidoglycan into the lateral cell wall. Each of these molecular machines contains penicillin-binding proteins (PBPs), which catalyze the final stages of peptidoglycan synthesis, plus a number of accessory proteins. Much effort has been made to identify these accessory proteins and determine their function. In the present paper we have used a novel approach to identify members of the pneumococcal elongasome that are functionally closely linked to PBP2b. We discovered that cells depleted in PBP2b, a key component of the elongasome, display several distinct phenotypic traits. We searched for proteins that, when depleted or deleted, display the same phenotypic changes. Four proteins, RodA, MreD, DivIVA and Spr0777, were identified by this approach. Together with PBP2b these proteins are essential for the normal function of the elongasome. Furthermore, our findings suggest that DivIVA, which was previously assigned as a divisomal protein, is required to correctly localize the elongasome at the negatively curved membrane region between the septal and lateral cell wall.

Introduction

Streptococcus pneumoniae is an important human pathogen with remarkable adaptation capabilities. It is a leading cause of community-acquired infections, including bacterial pneumonia, bacteremia, meningitis and otitis media. Thus, the threat of increasing β-lactam-resistance among pneumococci has become a major concern worldwide. Resistance to β-lactams in this bacterium is mediated by mosaic genes encoding altered penicillin-binding proteins (PBPs) with lower affinities for β-lactams than their corresponding native versions (Dowson *et al*., 1993; Sibold *et al.*, 1994). PBPs catalyze the late steps in peptidoglycan biosynthesis, i.e. the transglycosylase and transpeptidase reactions responsible for glycan chain elongation and crosslinking, respectively (Sauvage *et al*., 2008; Zapun et al., 2008; Egan *et al.,* 2015). The resulting peptidoglycan sacculus is a giant macromolecule that provides strength to withstand turgor pressure, and serves as a scaffold for cell wall-anchored components. The construction and preservation of this structure involve a large number of enzymes, transporters and cytoskeletal elements that interact in a complex and largely unknown manner (Zapun *et al*., 2008; Massidda *et al*., 2013; Philippe *et al*., 2014). The peptidoglycan layer consists of glycan chains composed of alternating repeats of N-acetylglucosamine (NAG) and N-acetylmuramic acid (NAM) interlinked by short peptide bridges. In *S. pneumoniae*, linear (unbranched) pentapeptides (L-alanyl-γ-D-glutamyl-L-lysyl-D-alanyl-D-alanine) attached to NAM residues on separate glycan strands are connected by formation of a direct bond between L-lysine at position 3 on one peptide stem and D-alanine at position 4 on the other (Vollmer *et al*., 2008). In addition to peptide bridges consisting only of cross-linked linear peptides, a considerable fraction of the bridges in pneumococcal peptidoglycan contains branched stem peptides. In branched stem peptides, a dipeptide branch consisting of L-alanine or L-serine followed invariably by L-alanine is appended to the ε-amino

terminus of L-lysine (Vollmer *et al*., 2008). The sequential addition of L-alanine/L-serine and L-alanine to the ε-amino group of L-lysine is carried out by MurM and MurN, respectively, and takes place at the cytoplasmic side of the membrane and (Filipe *et al.*, 2000).

S. pneumoniae produces six different PBPs: PBP1a, PBP1b, PBP2a, PBP2x, PBP2b and PBP3. The three class A enzymes (PBP1a, PBP1b and PBP2a) are bifunctional, having both transpeptidase and transglycosylase activity, while the class B PBPs (PBP2x and PBP2b) are monofunctional and possess only transpeptidase activity (Sauvage *et al*, 2008; Zapun *et al*.; 2008). In contrast to the five cell wall-synthesizing PBPs described above, the D,D-carboxypeptidase PBP3 regulates the extent of cross linking in peptidoglycan. It removes the terminal D-Ala residue from pentapeptides side chains to reduce the availability of donor stem-peptides for the transpeptidase reaction (Hakenbeck and Kohiyama, 1982; Abdullah *et al*., 2014). Mutants in which the genes encoding PBP1a, PBP1b or PBP2a have been deleted are viable, demonstrating that individually these PBPs are not essential for growth in the laboratory. PBP1b/PBP2a and PBP1a/PBP1b double deletion mutants can also be isolated. In contrast, a PBP1a/PBP2a double deletion as well as PBP2x and PBP2b single deletions are lethal (Kell *et al*., 1993; Paik *et al*., 1999; Berg *et al*., 2013).

Pneumococci are neither rods nor cocci, but have an intermediate ovoid shape (Philippe *et al.*, 2014). As the shape of bacteria depends on the shape of their peptidoglycan sacculus, the morphogenesis of *S. pneumoniae* requires septal as well as lateral peptidoglycan synthesis. The former is mediated by the divisome, while the latter involves a protein complex termed the elongasome (Zapun *et al*., 2008; Sham *et al*., 2012; Massidda *et al*., 2013). The composition, architecture, regulation and exact function of these molecular machines have been the subject of intense research for decades, but there still remain many unsettled questions. Recent studies have

shown that PBP2x is essential for formation of the septal cross wall, while PBP2b is indispensable for lateral peptidoglycan synthesis (Berg *et al*., 2013; Land *et al*., 2013; Peters *et al*., 2014; Tsui *et al*., 2014). Hence, PBP2x and PBP2b can be used as markers for the divisome and elongasome, respectively. We have previously shown that depletion of PBP2x gives rise to elongated lemon-shaped cells that struggle to divide, while PBP2b depleted cells form extremely long chains of cells that are compressed in the direction of their long axes (Berg *et al*., 2013). Moreover, we found that the peptidoglycan of PBP2b-depleted cells has an altered stem peptide composition (Berg *et al*., 2013). Recently we discovered that in addition to the above mentioned phenotypical changes, PBP2b-depleted cells become hypersensitive to the peptidoglycan hydrolase CbpD during competence (present work).

It is generally believed that PBP2b depends on several accessory proteins to function properly (Massidda *et al.*, 2013). We reasoned that it should be possible to identify such accessory proteins by screening for mutants with a CbpD-hypersensitive phenotype. We succeeded in identifying four proteins that, when deleted or depleted, gave rise to CbpD-hypersensitive strains, namely: RodA, MreD, DivIVA and Spr0777. In sum, our results show that together with PBP2b these proteins are essential for the normal function of the pneumococcal elongasome.

Results

Hypersensitivity to the peptidoglycan hydrolase CbpD in PBP2b-depleted pneumococci

S. pneumoniae is a naturally transformable species. When induced to competence, pneumococci readily take up exogenous DNA and incorporate it into their genomes by homologous recombination. Competent pneumococci secrete a peptidoglycan hydrolase, CbpD, which kills and

lyses susceptible streptococci present in the same environment (Kausmally *et al*., 2005; Johnsborg *et al*., 2008). This predatory mechanism, called fratricide, has presumably evolved to enable competent pneumococci to capture DNA from closely related strains and species sharing the same niche. The integral membrane protein ComM, which is only produced during the competence period, protects competent cells from committing suicide (Håvarstein *et al*., 2006). *comM* and *cbpD* belong to the early and late competence genes, respectively. Thus, transcription of the *cbpD* gene is delayed by at least 5 minutes compared to *comM*. The mechanism by which ComM protects against self-lysis is still not understood (Straume *et al*., 2015).

When inducing PBP2b-depleted pneumococci to competence we discovered that they start to lyse, meaning that they are no longer able to protect themselves against CbpD even though they possess a fully functional *comM* gene. To gradually deplete the transcription of the essential *pbp2b* gene, we used a previously described depletion system called ComRS (Berg *et al*., 2011; Berg *et al*., 2013). The system consists of a synthetic 8-amino acid peptide (ComS), a transcriptional activator (ComR) and a promoter (P_{comX}) containing a binding site for activated ComR. P_{comX} and the constitutively expressed *comR* gene were inserted into neutral sites in the pneumococcal genome. The level of expression of genes inserted behind P_{comX} can be fine-tuned by varying the concentration of ComS in the growth medium. ComS is imported into the cytoplasm by the AmiA oligopeptide permease. Once inside the cell, it binds to and activates ComR. To be able to manipulate the expression of PBP2b, a strain was constructed in which the *pbp2b* gene was placed behind the P_{comX} promoter. Next, the native *pbp2b* gene was deleted in this strain. Due to its essentiality, PBP2b was expressed ectopically from the P_{comX} promoter during the two transformation steps required to remove the native *pbp2b* gene with a so-called Janus cassette (Sung *et al*., 2001). To examine ComM-mediated immunity in the resulting strain, SPH157 (Table

130 1), depletion of PBP2b was performed as described previously (Berg *et al*., 2011; Berg *et al*.,
131 2013). Briefly, a culture of SPH157 cells grown in C medium containing 0.02 µM ComS was
132 washed once in C medium without ComS, and then serially diluted 2-fold in the same ComS-free
133 medium in a 96-well microplate with a clear bottom. The microplate was placed inside a Synergy
134 H1 Hybrid reader (BioTek, Winooski,VT, USA) at 37 ^{0}C. When reaching an OD_{492} ~ 0.2 the
135 culture was induced to competence by addition of 250 ng ml^{-1} of the competence stimulating
136 peptide (CSP). In order to measure cell lysis resulting from loss of ComM-mediated protection
137 against CbpD, the cells were grown in the presence of 2 µM Sytox green. Sytox green is a non-
138 toxic, membrane-impermeable dye that fluoresces 1000 times more brightly when bound to nucleic
139 acid. Following competence induction to activate expression of ComM and CbpD, a strong
140 increase in fluorescence was detected in PBP2b-depleted cultures (Fig. 1c). The increase in
141 fluorescence is caused by binding of Sytox green to DNA released from disintegrated cells. As
142 shown in Fig. 1c, a large fraction of the PBP2b-depleted cells lysed, demonstrating that they are
143 no longer protected by ComM.

144

145 ***Screening for proteins on which PBP2b is functionally dependent***

146 We reasoned that PBP2b requires the assistance of other proteins to function properly, and
147 that deletion or depletion of such accessory proteins would give rise to the same CbpD-
148 hypersensitive phenotype as observed for PBP2b-depleted cells. If so, this approach could be used
149 to screen for proteins on which PBP2b is functionally dependent. Targets were selected among
150 proteins previously reported to be involved in pneumococcal cell division and/or elongation
151 (Massidda *et al*, 2013; Fenton *et al*., 2015). Genes were deleted using the Janus cassette, or
152 depleted as described for PBP2b above. The results presented in Table 2 show that depletion of

RodA and Spr0777 leads to loss of ComM-mediated immunity against CbpD. When competence was induced in cultures of RodA (strain SPH354) and Spr0777 (strain SPH355) depleted cells, extensive cell lysis was observed (Fig. 1f and g). The same result was obtained with mutants in which the genes encoding MreD (strain SPH351) and DivIVA (strain SPH361) had been deleted (Table 2 and Fig. 1d and e). In contrast, no significant increase in cell lysis was observed in competence induced strains in which PBP1a, PBP2a, PBP1b, PBP2x, MreC, GpsB, FtsW, StkP, MurJ, MltG, MapZ, RodZ, FtsB, Pmp23 or Spr1357 had been deleted or depleted (Table 2). All strains that tested negative in the lysis assay were transformed with genomic DNA containing a novobiocin marker to verify that they develop the competent state when induced by CSP. In all cases the transformation efficiency was the same as that of the wild-type R6 strain (results not shown). This demonstrates that CbpD, ComM and the other competence genes are expressed normally in these strains. To verify that the strong autolytic response observed in competence-induced cells deficient in PBP2b, RodA, Spr0777, MreD or DivIVA is caused by CbpD, we deleted the *cbpD* gene in each of the strains (SPH157, SPH354, SPH355, SPH351 and SPH361) used in the experiments presented in Fig. 1. No lysis was detected when cultures of the resulting strains were induced to competence, demonstrating that the autolytic response depends on the muralytic activity of CbpD (Fig. S1). As a further control, we deleted the *comM* gene in SPH164 (P_{comX}::*pbp2x*), SPH344 (Δ*pbp1a*), SPH350 (Δ*mreC*) and SPH353 (P_{comX}::*gpsB*), four of the strains that tested negative in the autolysis assay (see Table 2). This was done to verify that the absence of competence-induced lysis in these strains is due to an intact ComM-mediated immunity mechanism that protects the cells against CbpD. Induction of competence in the resulting *comM*-deficient strains, which were assayed in exactly the same way as their parental strains, showed that they lysed like normal Δ*comM* mutants (results not shown).

CbpD-hypersensitive mutant strains have altered cell morphology

In addition to their CbpD-hypersensitivity, PBP2b-depleted cells display other characteristic features. They form very long chains of compressed lentil-shaped cells that are unable to split their septal cross walls (Berg *et al.*, 2013 and Fig. 2). If PBP2b cannot function normally without the assistance of RodA, Spr0777, MreD or DivIVA, it would be expected that deletion or depletion of these proteins would give rise to a PBP2b-like morphology. The results shown in Fig. 2 show that this is indeed the case. The MreD (SPH351) and DivIVA (SPH361) deletion mutants, as well as the strain depleted in RodA (SPH354), exhibited a change in morphology very similar to that of PBP2b-depleted cells. Spr0777 (SPH355) depleted cells also formed long chains of cells, but their shape were not consistently lentil-shaped as a minor portion of the cells had a more elongated form. In the case of DivIVA our results are in accordance with previous studies which have reported that pneumococcal mutants lacking this protein form chains (Fadda *et al*., 2007; Fleurie *et al*., 2014). In the case of MreD, however, previous studies have reported that a *S. pneumoniae* R6 strain in which MreD has been deleted displays a normal morphology (Land and Winkler, 2011).

Characterization of strains carrying mutated variants of DivIVA

DivIVA proteins from Gram-positive bacteria vary in size (Oliva *et al*., 2010). The N-terminal ~160 amino acids are relatively conserved, while the C-terminal part varies in length between species and is much less conserved. The *Bacillus subtilis* version of DivIVA consists only of the conserved part (164 aa), while the pneumococcal protein contains an additional C-terminal tail of

~100 amino acids. We wondered whether this C-terminal tail might be involved in protein-protein interactions involving other members of the elongasome. Hence, we made C-terminally truncated variants of pneumococcal DivIVA, and tested the mutants carrying the truncated proteins for morphological changes and loss of ComM-mediated immunity against CbpD. No changes in morphology or CbpD-sensitivity were observed with versions of DivIVA in which the C-terminal 40, 65 and 74 amino acids had been removed (Table 3). In comparison, removal of the 92 C-terminal amino acids (DivIVA-Δ92) gave rise to cells that formed long chains. ComM-mediated immunity to CbpD, however, was mostly intact in these cells. Interestingly, removal of the 112 C-terminal amino acids of DivIVA (DivIVA-Δ112) gave rise to long-chain pneumococci that in addition had lost immunity and become hypersensitive to CbpD. In other words, the strain expressing the DivIVA-Δ112 protein displays the same phenotype as the ΔDivIVA strain (Table 3).

It has been shown previously that DivIVA, which targets negatively-curved membranes (Lenarcic *et al*., 2009), localizes to the septal region and the poles of *S. pneumoniae* (Fadda *et al*., 2007). To determine whether DivIVA-Δ92 and DivIVA-Δ112 localize normally, they were tagged with green fluorescent protein (GFP) at their C-termini and examined by fluorescence microscopy. The results showed that DivIVA-Δ92-GFP and the "wild-type" protein (DivIVA-GFP) localize to the septum and poles. The DivIVA-Δ112-GFP protein, on the other hand, had lost the ability to target these regions, and was found to be dispersed throughout the cytoplasm (Fig. 3). Addition of the GFP-domain to wild-type DivIVA altered the morphology of the host cells. They formed chains, but not as long as the chains formed by ΔDivIVA mutants. This demonstrates that the presence of GFP affects the function of the DivIVA protein. Nevertheless, cells expressing DivIVA-GFP, as well as the DivIVA-Δ92-GFP protein, were still immune to CbpD when induced

to competence. In contrast, cells expressing DivIVA-Δ112-GFP lysed upon competence induction, demonstrating that loss of DivIVA-localization causes loss of CbpD-immunity.

Phosphoproteome analyses have revealed that pneumococcal DivIVA is phosphorylated at threonine 201 by the Ser/Thr protein kinase StkP (Sun *et al*. 2010, Nováková *et al*., 2010). To determine whether this phosphorylation affects chain length or CbpD-sensitivity we substituted T201 with an alanine or a glutamate. The former mutation removes the phosphorylation site, while the latter is a phosphomimetic mutation. The resulting strains, $DivIVA_{T201A}$ and $DivIVA_{T201E}$, displayed wild-type morphologies, and were immune to CbpD upon competence induction (data not shown).

Analysis of stem peptide composition

We have previously reported that pneumococci depleted in PBP2b incorporate a considerably higher proportion of branched stem peptides in their peptidoglycan than wild-type cells, whereas depletion of PBP2x does not affect the stem peptide composition (Berg *et al*., 2013). To determine the effect of deleting or depleting the PBP2b accessory proteins identified above, we analyzed the stem peptide composition of the ΔDivIVA (SPH361) and ΔMreD (SPH351) strains, and the strains depleted in RodA (SPH354) and Spr0777 (SPH355). Purified peptidoglycan from each strain was treated with LytA to release the stem peptides. To separate the peptides, the digested samples were analyzed by reversed-phase HPLC. The resulting stem peptide profiles are shown in Figure 4A. Peak I in the different panels represents a tetra-tri dimer in which L-Lys (position 3) on one peptide stem is directly linked to D-Ala (position 4) on the adjacent peptide stem (Figure 4B). Peak II, on the other hand, represents a tetra(SA)tri dimer, where L-Lys (position 3) and D-Ala (position 4)

are indirectly linked by a Ser-Ala interpeptide bridge (Fig. 4B). Since synthesis of a tetra(SA)tri dimer involves a branched lipid II precursor, whereas synthesis of a tetra-tri dimer does not, the ratio of material eluted in the two peaks (area peak I/ area peak II) can be used to compare the level of branched stem peptides in different mutant strains. A peak I/II ratio of 2.6 was calculated for the RH1 wild-type strain. This ratio, and the ratios given below, represent the mean of two independent experiments (see Supporting Information, Table S2). Upon depletion of PBP2b this ratio changes to 0.8, reflecting a strong increase in the incorporation of branched stem peptides. The corresponding peak ratios for RodA and Spr0777-depleted strains were 1.2 and 1.7, respectively. Thus, as for PBP2b, depletion of these proteins stimulates the incorporation of branched stem peptides. Similarly, the peptidoglycan of the ΔMreD strain (peak ratio = 1.7) contained a significantly higher amount of branched stem peptides than the RH1 wild type strain, while the increase was more modest in the ΔDivIVA strain (peak ratio = 2.2).

Analysis of peptidoglycan from cells in which ectopic PBP2b expression was driven by 0.02 µM ComS inducer revealed a peak ratio of 2.2. This is close to wild-type, but a ComS concentration of 0.02 µM might be a bit too low to induce normal expression levels of PBP2b, resulting in a reduced peak ratio compared to wild type. However, when adding 2 µM ComS to the growth medium to overexpress PBP2b, a peak ratio of 3.2 was obtained. It follows from this that overexpression of PBP2b leads to an increase in the relative content of unbranched stem peptides in pneumococcal peptidoglycan. In contrast to PBP2b, overexpression of RodA (2 µM ComS inducer) strongly reduced the growth rate of the cells. We therefore reduced the ComS concentration to 0.05 µM to obtain a roughly normal growth rate, and compared the stem peptide composition in cells grown under these conditions to RodA depleted cells (Figure 4A). Intriguingly, the peak ratio obtained with these cells was 3.2, compared to 1.2 in RodA depleted

cells. This result shows that supplementing the growth medium with 0.05 µM ComS leads to overexpression of RodA, and that the level of RodA expression strongly influences the stem peptide composition in *S. pneumoniae*. In the case of Spr0777, the control strain was grown in 0.2 µM ComS. A peak ratio of 2.2 was obtained when the peptidoglycan from these cells was analyzed (Figure 4A).

Bacterial two-hybrid analysis of PBP2b, RodA, MreD, DivIVA and Spr0777 interactions

The results presented above show that deletion or depletion of PBP2b, RodA, MreD, DivIVA and Spr0777 give rise to very similar phenotypic alterations with respect to three different traits. This represents strong evidence that the activity of these proteins are functionally linked. To investigate whether they are physically associated as well, we used the BACTH two-hybrid system to screen for protein-protein interactions (see Experimental Procedures). The BACTH system is based on the functional complementation of T18 and T25, two domains of the *Bordetella pertussis* adenylate cyclase (Karimova *et al*., 1998). For each pair of proteins to be tested, one protein is fused to T18, while the other is fused to T25. The resulting fusion proteins are then coexpressed in an *Escherichia coli cya*⁻strain. Positive interactions restore adenylate cyclase activity and result in cAMP synthesis followed by cAMP/CAP activated expression of β-galactosidase. To estimate the level of β-galactosidase activity in *E. coli* cells expressing the fusion proteins to be tested, they are spotted on LB plates containing X-gal. The appearance of dark blue colonies indicate strong protein-protein interactions, while weaker interactions give rise to light blue colonies. White colonies indicate non-interacting proteins. Our results show that PBP2b forms a homodimer and that it interacts strongly with RodA (Fig. 5). Clear positive reactions were also obtained with *E.*

coli cells expressing combinations of T25-PBP2b/T18-DivIVA and T18-PBP2b/MreD-T25, demonstrating that PBP2b interacts with DivIVA as well as MreD. Positive, although weaker signals, were observed with cells expressing combinations of T25-PBP2b/Spr0777-T18 and Spr0777-T18/MreD-T25. Furthermore, DivIVA interacts strongly with itself and with the Spr0777 protein. As negative controls we included empty plasmids (pKT25 and pUT18C) and the two protein pairs T25-PBP2b/Spr1357-T18 and T25-PBP2x/T18-RodA (Fig. 5).

Discussion

PBP2b and its accessory proteins are essential components of the elongasome

In the present study, we have searched for proteins that are functionally closely associated with PBP2b. We screened for proteins that upon deletion or depletion give rise to phenotypic alterations typical for PBP2b-depleted cells. These alterations include: i) loss of ComM-mediated immunity against the peptidoglycan hydrolase CbpD, ii) formation of long chains of longitudinally compressed cells, and iii) increased levels of branched muropeptides in the cell wall. Deletion/depletion of a number of proteins reported to be involved in septal or lateral peptidoglycan synthesis identified four proteins with the properties listed above, namely DivIVA, MreD, RodA and Spr0777. The unique phenotypic traits shared by cells depleted in PBP2b, DivIVA, MreD, RodA and Spr0777, provide strong evidence that these five proteins cooperate to build a functional elongasome.

To investigate whether PBP2b and its accessory proteins are in physical contact, we used the BACTH two-hybrid system. As shown in Fig. 5, PBP2b interacts strongly with RodA. Furthermore, we found significant interactions between PBP2b and MreD, and between PBP2b

and DivIVA. The β-galactosidase activity generated by the *E. coli* cells co-expressing the PBP2b and Spr0777 fusion proteins was relatively weak, but clearly above the negative controls. Hence, in sum, our results indicate that RodA, MreD, DivIVA, and probably also Spr0777, interact with PBP2b *in vivo*.

DivIVA is required for correct localization of the elongasome

It is well established in the literature that MreB, MreC, MreD, RodA as well as certain PBPs are required for cell elongation in rod-shaped bacteria (Jones *et al.*, 2001; Stewart, 2005; den Blaauwen *et al.*, 2008). Individual inactivation of these proteins cause rod-shaped cells to round up and form spheroids. Ovoid bacteria like *S. pneumoniae* also elongate during growth, but to a lesser extent. Although rod-shaped and ovoid bacteria share some of the proteins required for lateral peptidoglycan synthesis, there is clearly major differences. One important difference is that MreB is absent in ovococci (Daniel and Errington, 2003; Philippe *et al*., 2014). Members of the MreB family are actin homologues that assemble into helical filaments situated close to the inside of the cytoplasmic membrane (Jones *et al.,* 2001; van den Ent *et al*., 2001). This cytoskeleton directs lateral peptidoglycan synthesis during growth of rod-shaped bacteria by positioning the cell wall elongation machinery. In rod-shaped cells, the machinery inserts new cell wall material throughout the cylindrical part of the cell in a helical MreB-associated pattern (den Blaauwen *et al.*, 2008). In contrast, the pneumococcal elongation machinery seems to be located close to the septal region. Evidence for this is based on the fact that PBP2b, a key component of this machinery, is located in the septal area (Morlot *et al*., 2003; Land *et al*., 2013; Tsui *et al*., 2014). Since MreB is absent in *S. pneumoniae*, a different mechanism must operate to position the proteins involved in lateral peptidoglycan synthesis. DivIVA has previously been associated with the divisome

(Massidda *et al*., 2013; Fadda *et al*., 2007). Immunolocalization studies by Fadda *et al*. (2007) demonstrated that DivIVA localizes to the septal region as well as the poles in *S. pneumoniae* (Fadda *et al.*, 2007). This was confirmed by immunogold labeling, which revealed that DivIVA localizes to the regions of the cell with the strongest negatively curved membrane regions, i.e. the cell poles and the edge where the division septum meets the periphery of the cell (Fadda *et al*., 2007). In the present study, we used a novel approach based on shared phenotypic traits to show that DivIVA is part of the pneumococcal elongation machinery. We also discovered that DivIVA interacts strongly with Spr0777 in the BACTH two-hybrid assay, suggesting that DivIVA is recruited to the elongasome by Spr0777. Furthermore, DivIVA truncation experiments revealed that loss of elongasome function is closely associated with loss of DivIVA localization. Together, our results, and those of previous localization studies, represent strong evidence that: i) DivIVA is needed to correctly localize the pneumococcal elongation machinery, and ii) this machinery is positioned at the highly negatively curved membrane region between the septal and lateral cell wall.

In a recent paper, Fleurie *et al.* (2014) proposed that GpsB and DivIVA function as regulators of septal and lateral peptidoglycan synthesis in *S. pneumoniae*. According to their findings, one function of DivIVA might be to switch on lateral peptidoglycan synthesis to initiate cell elongation. Our results are not in conflict with this idea, as it is possible that DivIVA activates the cell elongation machinery by contributing to the correct assembly and localization of the elongasome. During synthesis of the septal cross wall, the divisome localizes in a ring at the leading edge of the constricting plasma membrane. Hence, the divisome and elongasome must be different entities that mostly operate at different locations in the cell. It is possible, however, that they form a single large complex at the initiation of cell division, i.e. when the septal cross wall

starts to form. Our model is in agreement with the findings of Tsui *et al.* (2014). They observed that, while PBP2x co-localizes with PBP2b during the early stages of cell division, PBP2x separates from PBP2b and moves to a central septal location at mid-to-late division.

PBP2b and RodA have a close functional relationship

FtsW, RodA and SpoVE belong to the SEDS (shape, elongation, division and sporulation) family of integral membrane proteins (Gérard *et al.*, 2002). FtsW has been reported to be a lipid II flippase that translocates this peptidoglycan precursor across the cytoplasmic membrane (Mohammadi *et al*., 2011). In *Escherichia coli*, FtsW is closely associated with a class B PBP termed PBP3 (FtsI), which corresponds to PBP2x in *S. pneumoniae* (Sauvage *et al*., 2008). FtsW has been shown to co-immunoprecipitate with PBP3 *in vitro*, and to interact with PBP3 in a two-hybrid assay (Karimova *et al*., 2005; Fraipont *et al.*, 2011). FtsW and PBP3 are both essential for septal peptidoglycan synthesis during cell division in *E. coli* (Boyle *et al*., 1997; Pastoret *et al*., 2004). Localization of FtsW to the divisome has also been demonstrated in *B. subtilis* and *S. pneumoniae* (Morlot *et al*., 2004; Gamba *et al*., 2009; Noirclerc-Savoye *et al*., 2013). Due to their sequence homology and topological equivalence, it is likely that FtsW and RodA have the same or similar functions in the bacterial cell (Ikeda *et al*., 1989; Gérard *et al*., 2002). Based on this, and other data (see below), it has been proposed that RodA is a lipid II flippase that specifically serves the cell-elongation machinery (Mohammadi *et al*., 2011; Massidda *et al*., 2013; Philippe *et al*., 2014). However, in two recent publications, the view that FtsW and RodA are important for lipid II translocation *in vivo* was challenged (Sham *et al*., 2014; Meeske *et al*., 2015). Several lines of evidence were presented suggesting that another protein, termed MurJ, is responsible for lipid II flippase activity in bacteria. MurJ-type flippases are members of the multidrug/oligosaccharidyl-

lipid/polysaccharide (MOP) exporter superfamily (Hvorup *et al*., 2003). MurJ is essential in *E. coli*, and depletion of the protein gives rise to cell-shape defects and eventually lysis. Unexpectedly, however, deletion of all 10 MOP superfamily members present in *B. subtilis* did not alter the bacterium's growth rate or cell morphology (Fay and Dworkin, 2009; Meeske *et al*., 2015). This puzzle was solved by the discovery that a previously uncharacterized protein, Amj, can substitute for YtgP, the MurJ ortholog in *B. subtilis* (Meeske *et al*., 2015). The genomes of *S. pneumoniae* and other streptococci encode a single MurJ ortholog, but lack the proposed Amj flippase (Meeske *et al*., 2015). Interestingly, MurJ from *Streptococcus pyogenes* is able to complement *E. coli* strains depleted in endogenous MurJ (Ruiz, 2009). Hence, it is reasonable to assume that pneumococcal MurJ (Spr1383), which is 56% identical to *S. pyogenes* MurJ at the amino acid sequence level, also functions as a lipid II flippase. Depletion of MurJ in *S. pneumoniae* strain R6 gave rise to elongated and sometimes lemon-shaped cells, reminiscent of the morphology observed for FtsW-depleted cells (results not shown). This, and the fact that competence-induced MurJ-depleted cells are still immune against CbpD, show that the functions of MurJ and PBP2b are not tightly associated.

RodA was first identified in *E. coli* as an essential protein that affects cell morphology (Matsuzawa *et al*., 1973). *E. coli* cells with non-functional *rodA* genes lose their characteristic rod-like shape and become spherical. Furthermore, it has been reported that RodA is required for the proper function of PBP2, a monofunctional transpeptidase essential for cell elongation and shape maintenance in *E. coli* (Ishino *et al*, 1986). Similarly, RodA and the monofunctional transpeptidases PBP2a and PBPH are essential components of the elongation machinery in *B. subtilis* (Henriques *et al*., 1998; Wei *et al*., 2003). Thus, in the model bacteria *E. coli* and *B. subtilis,* FtsW and RodA are essential and associated with the divisome and elongasome, respectively.

Interestingly, in *Streptococcus thermophilus* CNRZ368 deletion of either *pbp2b* or *rodA* is not lethal. However, in both cases disruption of the genes results in increased chain length and spherical instead of ovoid cells, suggesting a close functional relationship between PBP2b and RodA (Thibessard *et al.*, 2002). We observed the same close functional relationship between RodA and the elongasome-specific transpeptidase PBP2b in *S. pneumoniae*. Depletion of pneumococcal RodA gave rise to the same phenotypical changes as depletion of PBP2b, i.e. very long chains of lentil-shaped cells, increased incorporation of branched stem peptides, and hypersensitivity to CbpD. In addition, a strong interaction between RodA and PBP2b was detected in the BACTH two-hybrid assay (Fig. 5). In contrast, depletion of pneumococcal FtsW generated elongated and irregularly shaped cells that were resistant to CbpD-mediated cell lysis when induced to competence (data not shown). In sum, these results strongly indicate that there is an intimate functional relationship between PBP2b and RodA in *S. pneumoniae*.

During revision of the present work, a paper by Meeske *et al.* (2016) appeared that presented strong evidence that RodA and other members of the SEDS protein family are peptidoglycan polymerases. Based on this discovery it is reasonable to assume that MurJ, rather than the SEDS proteins FtsW and RodA, is the major lipid II flippase in *S. pneumoniae*. However, at present, it cannot be ruled out that SEDS proteins are both lipid II flippases and peptidoglycan polymerases. The unexpected finding that RodA is a peptidoglycan polymerase nicely explains the tight functional relationship between RodA and PBP2b, and presumably enables PBP2b to function independently of class A PBPs.

The functions of class A and B PBPs do not seem to be closely linked

In contrast to pneumococcal class B PBPs, class A PBPs can to a large extent substitute for each other. The exception is PBP1b, which cannot substitute for the concomitant loss of PBP1a and PBP2a. Unexpectedly, individual deletion of PBP1a, PBP2a or PBP1b, did not give rise to the PBP2b-specific phenotypical alterations described above. This demonstrates that PBP2b does not depend on any particular class A PBP to function normally, and supports the finding that RodA rather than a class A PBP is the peptidoglycan polymerase that operates in conjunction with PBP2b to synthesize the lateral cell wall (Meeske *et al*., 2016). By analogy, it is likely that PBP2x and FtsW work together in the divisome to synthesize the septal cross-wall. The notion that class A and B PBPs operate independently of each other in the elongasome as well as the divisome machinery is also supported by studies demonstrating that PBP2x localizes separately from PBP1a during the later stages of cell division (Land *et al*., 2013; Tsui *et al*., 2014). If, as the evidence suggest, the function of class A and B PBPs are not closely linked, class A PBPs are probably part of other peptidoglycan synthesizing protein complexes. Hence, it is possible that *S. pneumoniae* contains a total of five independent peptidoglycan synthesizing machineries. Apart from the elongasome and divisome, which are built around PBP2b/RodA and PBP2x/FtsW, respectively, there could be separate machineries with partly overlapping functions for each class A PBP. Alternatively, the elongasome and divisome could contain class A as well as class B PBPs, but in separate subcomplexes. The elongasome, for instance, might consist of two subcomplexes that cooperate during lateral peptidoglycan synthesis: one built around PBP2b/RodA and the other around a class A PBP. If so, these subcomplexes probably operate in a coordinated but relatively independent manner.

The expression levels of PBP2b and RodA have a strong impact on the stem-peptide composition of the cell wall

When PBP2b is depleted in pneumococcal cells, the relative content of branched stem peptides in their peptidoglycan increases significantly compared to wild type cells. Overexpression of PBP2b (2 µM ComS), on the other hand, produce peptidoglycan with a significantly lower relative content of branched stem peptides than wild type cells and cells grown in the presence of 0.02 µM ComS (Fig 4A; Berg *et al*., 2013). Even though overexpression of PBP2b causes significant changes in the stem peptide composition, it seems to be well tolerated by the pneumococcal cells. The generation-time at 37 ^{0}C of exponentially growing cultures exposed to 0.02 and 2 µM ComS inducer is about 35 and 40 minutes, respectively. In comparison, the generation-time of wild-type *S. pneumoniae* R6 cells is about 35 minutes. Since PBP2b overexpression increases the ratio of unbranched to branched stem peptides, while depletion has the opposite effect, it appears that unbranched stem-peptides are the preferred substrate used in transpeptidation reactions catalyzed by PBP2b. Similarly, depletion of RodA gives rise to an increased proportion of branched stem peptides in the cell wall, while overexpression has the opposite effect. This suggests that unbranched lipid II is a better substrate for RodA than branched. In contrast to PBP2b, overexpression of RodA reduces the growth rate significantly. SPH354 cells grown in the presence of 0.05 µM ComS have a generation time of 35-40 minutes, while it increases to 60 minutes in the presence of 2 µM inducer peptide. It is possible that overexpression of RodA is deleterious to the cells because it leads to a strong increase in the synthesis of glycan strands, which due to the stoichiometric imbalance between RodA and PBP2b might not be incorporated correctly into the cell wall or remain unprocessed. Overexpression of PBP2b, on the

other hand, might be better tolerated because it primarily affects the extent of glycan strand cross-linking.

Deletion of MreC and MreD give rise to very different phenotypes

Land and Winkler (2011) reported that MreC and MreD are essential in *S. pneumoniae* strain D39, whereas both proteins can be deleted in the R6 strain. For this reason, they speculated that their R6 strain had acquired suppressors that compensated for the loss of MreCD. They also found that Δ*mreCD*, Δ*mreC* and Δ*mreD* knock-out mutants of their R6 strain grow like the parental strain and have normal cell morphology. In accordance with Land and Winkler (2011) we found that *mreC* and *mreD* can be deleted in our R6 strain. However, while the Δ*mreC* mutant grew well and had normal morphology (results not shown), the Δ*mreD* mutant grew very slowly and formed extremely long chains of lentil-shaped cells (see Fig. 2d). Moreover, we found that the Δ*mreD* mutant is hypersensitive to CbpD, while the Δ*mreC* mutant is immune (Table 2). The difference in phenotype between our Δ*mreC* and Δ*mreD* mutant strains was unexpected as the MreCD proteins have been reported to form a complex and consequently are believed to be functionally interconnected (Philippe *et al*., 2014). This led us to check whether MreC really is essential in the D39 strain. We got the same result as for the R6 strain, i.e. MreC is not essential in either strain. The stop codon of *mreC* overlaps with the start codon of *mreD.* Consequently, the Shine-Dalgarno (SD) sequence of the *mreD* gene is located at the 3'-end of the *mreC* gene. Thus, to avoid a polar effect on the expression of MreD, it is important not to delete the SD sequence together with the *mreC* gene. As far as we can tell, the Δ*mreC* mutant constructed by Land and Winkler (2011) lacks the SD sequence in front of the downstream *mreD*. Hence, it might be that a polar effect on MreD expression is the reason they identified MreC as essential in their D39 strain. In a recent paper,

García-Lara *et al*. (2015) reports that a *Staphylococcus aureus* Δ*mreC* mutant grows identically to the parental strain, while lack of MreD leads to growth defects and abnormal cell morphology. This is very similar to the phenotypes we observe for the pneumococcal *mreC* and *mreD* mutants.

Spr0777 - a conserved protein of unknown function

Similar to MreD, Spr0777 is an integral membrane protein of unknown function. It was identified by transposon mutagenesis and high-throughput sequencing (Tn-seq analysis) as a new cell wall biogenesis factor in *S. pneumoniae* (Fenton *et al*., 2015). Spr0777 is predicted to contain eight transmembrane segments and a large extracellular loop of about 60 amino acids. Homologs of Spr0777 are widespread among Gram-positive as well as Gram-negative bacteria, suggesting that they serve an important function (Rettner and Saier, 2010). The *ydgG* gene of *E. coli* encodes a Spr0777 homolog that, when deleted, gives rise to increased biofilm thickness in flow cells. It was proposed that YdgG controls biofilm formation by acting as a transporter of the quorum-sensing signal AI-2 (Herzberg *et al.*, 2006). Later studies, however, have cast doubt on this theory (De Araujo *et al*., 2010; Pereira *et al*., 2013). Our finding that depletion of Spr0777 strongly affects the stem peptide composition in pneumococci, suggests that deletion of YdgG in *E. coli* may alter biofilm formation by introducing structural changes in the cell wall or outer surface of the cells. The fact that depletion of Spr0777 gives rise to phenotypical changes very similar to those observed for PBP2b-depleted cells, shows that PBP2b depends on Spr0777 to function properly. Moreover, our finding that Spr0777 interacts strongly with DivIVA (Fig. 5) indicates that Spr0777 is required for the correct subcellular localization of the elongasome. In addition, Spr0777 might be important for the spatial organization of the elongasome, or be involved in regulating its activity during the cell cycle. The genome of *S. pneumoniae* contains a homolog of Spr0777 with the same

topology (Spr1357). In contrast to Spr0777, Spr1357 is not essential in strain R6, and depletion of the Spr1357 protein did not generate any of the phenotypic changes characteristic of PBP2b-depleted cells.

A better understanding of the composition and function of the pneumococcal elongasome is not only of great academic interest, but could also have important clinical implications. The bacterial cell wall biosynthesis machinery has been, and still remains, a gold mine of potential drug targets. Hence, it is likely that increased knowledge in this field will provide new perspectives and ideas that will help researchers select the best targets for future drug development.

Experimental Procedures

Cultivation and transformation of S. pneumoniae

Strains of *S. pneumoniae* used in this study are listed in Table 1. *S. pneumoniae* was grown in C medium (Lacks and Hotchkiss, 1960) at 37°C. Selection for *S. pneumoniae* transformants was performed anaerobically on Todd-Hewitt agar plates containing the appropriate antibiotics at the following concentrations: kanamycin (400 µg ml^{-1}), streptomycin (200 µg ml^{-1}), spectinomycin (200 µg ml^{-1}) and novobiocin (2.5 µg ml^{-1}). When necessary, ComS inducer was added to the growth medium to drive ectopic expression of specific genes. Gene depletion experiments were done by removing the ComS inducer from the growth medium as described by Berg *et al.* (2011).

To construct mutant strains, DNA was introduced into the genome of *S. pneumoniae* by natural transformation. When pneumococcal cultures reached OD_{550} = 0.05- 0.1, transforming DNA and 250 ng ml^{-1} of synthetic competence stimulating peptide (CSP-1) were added. The

cultures were incubated at 37°C for 120 minutes before transformants were selected on Todd-Hewitt agar plates.

Construction of mutants

Genetic knockouts or the introduction of other mutations in the *S. pneumoniae* genome were made by transforming *S. pneumoniae* with antibiotic resistance markers or cassettes containing genetically modified target genes. The DNA cassettes were constructed by overlap extension PCR (Higuchi *et al.*, 1988) following the same protocol as described in previous publications (Berg *et al.*, 2013, Johnsborg *et al.*, 2008). All primers used in this work are listed in the supplementary Table S1. Briefly, to create genetic knockouts the ~1000 bp region upstream and downstream of a target gene were fused to the 5' and 3' end, respectively, of a desired antibiotic resistance gene by overlap extension PCR. This amplicon was then transformed into *S. pneumoniae* to knock out the target gene by homologous recombination. In this study the majority of mutants were created by using the Janus system (Sung *et al.*, 2001), which allows insertion and deletion of the Janus in a streptomycin resistant background. Knockout mutants were screened by PCR and all mutations that were introduced in the genome of *S. pneumoniae* were confirmed by sequencing.

Sytox assay

Cell lysis of *S. pneumoniae* cultures was monitored in real time by growing the cells in the presence of Sytox Green Nucleic Acid Stain (Invitrogen™) as previously described by Straume *et al.*, (2015). Sytox fluoresces strongly upon binding DNA when excited at 485 nm. As it is unable to cross the cytoplasmic membrane, fluorescence signal will only occur when Sytox binds to DNA

559 derived from lysed cells. Cells were grown in the presence of 2 µM Sytox Green in 96-well
560 Corning NBS clear-bottom plates at 37°C. OD_{492} and light emitted at 528 nm was measured
561 separately every 5 minutes using a Synergy H1 Hybrid Reader (BioTek). At OD_{492} ~ 0.2 the
562 cultures were induced to competence by adding a final concentration of 250 ng ml^{-1} CSP.

563

564 ***Scanning electron microscopy and fluorescence microscopy***

565 For SEM analysis strain SPH361 (Δ*divIVA*), SPH351 (Δ*mreD*) and SPH350 (Δ*mreC*) were grown
566 to an OD_{550} = 0.3 and collected by centrifugation at 4000 *g*. Cells depleted for RodA (SPH354) or
567 Spr0777 (SPH355) were prepared using the ComRS gene depletion system (Berg *et al.*, 2011).
568 Gene depletion was performed by following the protocol described by Berg *et al*., (2013), except
569 that SPH354 was pre-grown in the presence of 0.05 µM ComS rather than 0.02 µM. Growth was
570 followed spectrophotometrically, and 10 ml samples were collected when the growth rate of the
571 *rodA*- or *spr0777*-depleted cells was severally inhibited compared to the ComS-induced control
572 cells. The collected cells were fixed and prepared for SEM analysis as previously described by
573 Berg *et al*., (2013).

574 Fluorescence microscopy of DivIVA-GFP, DivIVA92-GFP and DivIVA112-GFP was
575 done using a Zeiss LSM 700 confocal microscope. *S. pneumoniae* strains expressing the different
576 DivIVA GFP fusions from the native P_{divIVA} promoter were grown to OD_{550} = 0.2. Cells were then
577 withdrawn and immediately examined by fluorescence microscopy.

578

579

580 ***Purification of peptidoglycan and HPLC analysis***

581 Peptidoglycan was purified as previously described by Vollmer (2007). The material was isolated
582 from 1-2 L cultures of exponentially growing cells (OD_{550} = 0.4-0.5) or from gene depleted cells
583 for which growth were severally inhibited or had stopped (OD_{550} = 0.3-0.5). Stem peptides from
584 2 mg of peptidoglycan were released by incubation over night with 2.5 µg of the amidase LytA in
585 100 µl of 20 mM Na-phosphate buffer (pH 7.0). After LytA digestion, the enzyme was precipitated
586 by incubating the samples at 95°C for 20 minutes. After clarifying the samples by centrifugation
587 at 20 000 *g* for 20 minutes, pH was adjusted to 2-3 with 20% phosphoric acid. Cell wall stem
588 peptides were separated by HPLC using a Dionex Ultimate 3000 LC system. Peptide separation
589 was performed by injecting 40 µl cell wall digest into a C18 reverse phase column (Vydac 218TP
590 C18 5 µm, Grace Davison Discovery Sciences). The peptides were eluted using a linear 120-
591 minutes gradient of acetonitrile from 0-15% starting with buffer A containing 0.05% trifluoracetic
592 acid (TFA) and finishing with buffer B containing 15% acetonitrile in 0.035% TFA. The flow-rate
593 was kept at 0.5 ml min^{-1}, and peptides were detected at 206 nm.
594

595 ***BACTH two-hybrid assay***

596 BACTH is a system developed for detecting interactions between two proteins, and is based on
597 the principle that if one protein being fused to a T18 domain interacts with another protein being
598 fused to a T25 domain, the T18 and T25 domains form a cAMP producing enzyme who's activity
599 can be detected. BACTH assays were performed as described by the manufacturer (Euromedex).
600 Plasmids containing the relevant T18/T25 fusions of *pbp2b, rodA, mreD, spr0777, divIVA,*
601 *spr1357* and *pbp2x* were isolated from *E. coli* X1-Blue cells (See supplemental material for
602 primers, plasmids and restriction enzymes used to construct the T18/T25 fusions). Combinations

603 of these plasmids were then co-transformed (one expressing a T18-fused protein and the other
604 expressing a T25-fused protein) into the expression cells *E. coli* BTH101 (Euromedex).
605 Transformants were selected on LB agar plates containing both 100 µg ml^{-1} ampicillin and 50 µg
606 ml^{-1} kanamycin. The transformants were grown to OD_{600} = 0.4-0.5 at 37 °C with shaking, before
607 2.5 µl of the cell culture was spotted onto LB agar plates containing 100 µg ml^{-1} ampicillin, 50
608 µg ml^{-1} kanamycin, 0.5 mM IPTG (Promega) and 40 µg ml^{-1} of X-gal (Promega). The plates were
609 incubated over night at 30 °C, protected from light. Bacterial spots that appeared blue were
610 regarded as a positive interaction between the two proteins fused to the T18 and T25 domains.
611 Each protein-protein interaction experiment was repeated three times.

612

613 ## Abbreviated Summary

614 In the present paper we show that deletion or depletion of PBP2b, RodA, MreD, DivIVA or
615 Spr0777 induce very similar phenotypic changes in *Streptococcus pneumoniae* strain R6,
616 providing strong evidence that these proteins cooperate to build a functional elongasome. DivIVA
617 targets negatively curved membranes. It is therefore likely that the function of DivIVA is to
618 correctly localize the elongasome at the highly negatively curved membrane region between the
619 septal and lateral cell wall.

620

621

622

623

Acknowledgements

We thank Hilde Raanaas Kolstad at the Imaging Centre at the Norwegian University of Life Sciences for technical assistance with the SEM analysis. The study was supported by The Research Council of Norway.

Author Contributions

(i) The conception or design of study: DS, GAS, KHB, LSH

(ii) The acquisition, analysis or interpretation of data: DS, GAS, KHB, ZS, LSH

(iii) Writing of the manuscript: DS, GAS, LSH

References

Abdullah, M.R., Gutiérrez-Fernández, J., Pribyl, T., Gisch, N., Saleh., M., Rohde, M., *et al*. (2014) Structure of the pneumococcal L,D-carboxypeptidase DacB and pathophysiological effects of disabeled cell wall hydrolases DacA and DacB. Mol Microbiol **93:** 1183-1206.

Berg, K.H., Biørnstad, T.J., Straume, D., and Håvarstein, L.S. (2011) Peptide-regulated gene depletion system developed for use in *Streptococcus pneumoniae*. J Bacteriol **193:** 5207-5215.

642 Berg, K.H., Stamsås, G.A., Straume, D., and Håvarstein, L.S. (2013) Effects of low PBP2b levels
643 on cell morphology and peptidoglycan composition in *Streptococcus pneumoniae*. J
644 Bacteriol **195:** 4342-4354.

645 Boyle, D.S., Khattar, M.M., Addinall, S.G., Lutkenhaus, J., and Donachie, W.D. (1997) *ftsW* is an
646 essential cell-division gene in *Escherichia coli*. Mol Microbiol **24:** 1263-1273.

647 Cato, A., Jr. and Guild, W.R. (1968) Transformation and DNA size. I. Activity of fragments of
648 defined size and a fit to a random double cross-over model. J Mol Biol **37**: 157-178.

649 Daniel, R.A., and Errington, J. (2003) Control of cell morphogenesis in bacteria: two distinct ways
650 to make a rod-shaped cell. Cell **113:** 767-776.

651 De Araujo, C., Balestrino, D., Roth, L., Charbonnel, N., and Forestier, C. (2010) Quorum sensing
652 affects biofilm formation through lipopolysaccharide synthesis in *Klebsiella pneumoniae*.
653 Res Microbiol **161:** 595-603.

654 den Blaauwen, T., de Pedro, M.A., Nguyen-Distèche, M., and Ayala, J.A. (2008) Morphogenesis
655 of rod-shaped sacculi. FEMS Microbiol Rev **32:** 321-344.

656 Dowson, C.G., Coffey, T.J., Kell, C., and Whiley, R.A. (1993) Evolution of penicillin resistance
657 in *Streptococcus pneumoniae*; the role of *Streptococcus mitis* in the formation of a low
658 affinity PBP2B in *S. pneumoniae.* Mol Microbiol **9:** 635-643.

659 Egan, A.J.F., Biboy, J., van't Veer, I., Breukink, E., and Vollmer, W. (2015) Activities and
660 regulation of peptidoglycan synthases. Phil Trans R Soc B **370:** 20150031.

661 Eldholm, V., Johnsborg, O., Haugen, K., Solheim-Ohnstad, H., and Håvarstein, L.S. (2009)
662 Fratricide in *Streptococcus pneumoniae*: contributions and role of the cell wall hydrolases
663 CbpD, LytA and LytC. Microbiology **155:** 2223-2234.

664 Fadda, D., Santona, A., D'Ulisse, V., Ghelardini, P., Ennas, M.G., Whalen, M.B., *et al*. (2007)
665 *Streptococcus pneumoniae* DivIVA: Localization and interactions in a MinCD-free
666 context. J Bacteriol **189:** 1288-1298.

667 Fay, A., and Dworkin, J. (2009) *Bacillus subtilis* homologs of MviN (MurJ), the putative
668 *Escherichia coli* lipid II flippase, are not essential for growth. J Bacteriol **191:** 6020-6028.

669 Fenton, A., Bernhardt, T., and Rudner, D. (2015) Identification of new cell wall biogenesis factors
670 in *Streptococcus pneumoniae* using Tn-Seq. Pneumonia **7:** 54.

671 Filipe, S.R., Pinho, M.G., and Tomasz, A. (2000) Characterization of the *murMN* operon involved
672 in the synthesis of branched peptidoglycan peptides in *Streptococcus pneumoniae*. J Biol
673 Chem **275:** 27768-27774.

674 Fleurie, A., Manuse, S., Zhao, C., Campo, N., Cluzel, C., Lavergne, J.P., *et al.* (2014) Interplay of
675 the serine/threonine-kinase StkP and the paralogs DivIVA and GpsB in pneumococcal cell
676 elongation and division. PLoS Genet **10:** e1004275.

677 Fraipont, C., Alexeeva, S., Wolf, B., van der Ploeg, R., Schloesser, M., den Blaauwen, T., et al.
678 (2011) The integral membrane FtsW protein and peptidoglycan synthase PBP3 form a
679 subcomplex in *Escherichia coli*. Microbiology **157:** 251-259.

680 Gamba, P., Veening, J.W., Saunders, N.J., Hamoen, L.W., and Daniel, R.A. (2009) Two-step
681 assembly dynamics of the *Bacillus subtilis* divisome. J Bacteriol **191:** 4186-4194.

García-Lara, J., Weihs, F., Ma, X., Walker, L., Chaudhuri, R.R., Kasturiarachchi, J., *et al.* (2015) Supramolecular structure in the membrane of *Staphylococcus aureus*. Proc Natl Acad Sci USA **112**: 15725-15730.

Gérard, P., Vernet, T., and Zapun, A. (2002) Membrane topology of the *Streptococcus pneumoniae* FtsW division protein. J Bacteriol **184:** 1925-1931.

Hakenbeck, R., and Kohiyama, M. (1982) Purification of penicillin-binding protein 3 from *Streptococcus pneumoniae*. Eur J Biochem **127:** 231-236.

Herzberg, M., Kaye, I.K., Peti, W., and Wood, T.K. (2006) YdgG (TqsA) controls biofilm formation in Escherichia coli K-12 through autoinducer-2 transport. J Bacteriol **188:** 587-598.

Håvarstein, L.S., Martin, B., Johnsborg, O., Granadel, C., and Claverys, J.P. (2006) New insights into the pneumococcal fratricide: relationship to clumping and indentification of a novel immunity factor. Mol Microbiol **59:** 1297-1307.

Henriques, A.O., Glaser, P., Piggot, P.J., and Moran Jr, C.P. (1998) Control of cell shape and elongation by the *rodA* gene in *Bacillus subtilis*. Mol Microbiol **28:** 235-247.

Higuchi, R., von Beroldingen, C.H., Sensabaugh, G.F., and Erlich, H.A. (1988) DNA-typing from single hairs. Nature **332:** 543-546.

Hvorup, R.N., Winnen, B., Chang, A.B., Jiang, Y., Zhou, X.F., and Saier Jr, M.H. (2003) The multidrug/oligosaccharidyl-lipid/polysaccharide (MOP) exporter superfamily. Eur J Biochem **270:** 799-813.

Ikeda, M., Sato, T., Wachi, M., Jung, H.K., Ishino, F., Kobayashi, Y., *et al.* (1989) Structure similarity among *Escherichia coli* FtsW and RodA proteins and *Bacillus subtilis* SpoVE protein, which function in cell division, cell elongation, and spore formation, respectively. J Bacteriol 171: 6375-6378.

Ishino, F., Park, W., Tomioka, S., Tamaki, S., Takase, I., Kunugita, K., *et al*. (1986) Peptidoglycan synthetic activities in membranes of *Escherichia coli* caused by overproduction of penicillin-binding protein 2 and RodA protein. J Biol Chem **261:** 7024-7031.

Johnsborg, O., Eldholm, V., Bjørnstad, M.L., and Håvarstein, L.S. (2008) A predatory mechanism dramatically increases the efficiency of lateral gene transfer in *Streptococcus pneumoniae* and related commensal species. Mol Microbiol **69:** 245-253.

Johnsborg, O., and Håvarstein, L.S. (2009) Pneumococcal LytR, a protein from the LytR-CpsA-Psr family, is essential for normal septum formation in *Streptococcus pneumoniae*. J Bacteriol **191:** 5859-5864.

Jones, L.J.F., Carballido-López, R., and Errington, J. (2001) Control of cell shape in bacteria: helical, actin-like filaments in *Bacillus subtilis*. Cell **104:** 913-922.

Karimova, G., Pidoux, J., Ullmann, A., and Ladant, D. 1998. A bacterial two-hybrid system based on a reconstituted signal transduction pathway. Proc Natl Acad Sci USA **95**: 5752-5756.

Karimova, G., Dautin, N., and Ladant, D. (2005) Interaction network among *Escherichia coli* membrane proteins involved in cell division as revealed by bacterial two-hybrid analysis. J Bacteriol **187:** 2233-2243.

723 Kausmally, L., Johnsborg, O., Lunde, M., Knutsen, E., and Håvarstein, L.S. (2005) Choline-
724 binding protein D (CbpD) in *Streptococcus pneumoniae* is essential from competence-
725 induced cell lysis. J Bacteriol **187:** 4338-4345.

726 Kell, C.M., Sharma, U.K., Dowson, C.G., Town, C., Balganesh, T.S., and Spratt, B. (1993)
727 Deletion analysis of the essentiality of penicillin-binding proteins 1A, 2B, and 2X of
728 *Streptococcus pneumoniae*. FEMS Microbiol Lett **106:** 171-175.

729 Lacks, S., and Hotchkiss, R.D. (1960) A study of the genetic material determining an enzyme in
730 pneumococcus. Biochim Biophys Acta **39:** 508-518.

731 Land, A.D., and Winkler, M.E. (2011) The requirement for pneumococcal MreC and MreD is
732 relieved by inactivation of the gene encoding PBP1a. J Bacteriol **193:** 4166-4179.

733 Land, A.D., Tsui, H.C.T., Kocaoglu, O., Vella, S.A., Shaw, S.L., Keen, S.K., *et al.* (2013)
734 Requirement of essential Pbp2x and GpsB for septal ring closure in *Streptococcus*
735 *pneumoniae* D39. Mol Microbiol **90:** 939-955.

736 Lenarcic, R., Halbedel, S., Visser, L., Shaw, M., Wu, L.J., Errington, J., *et al*. (2009) Localisation
737 of DivIVA by targeting to negatively curved membranes. EMBO J **28:** 2272-2282.

738 Massidda, O., Novakova, L., and Vollmer, W. (2013) From models to pathogens: how much have
739 we learned about *Streptococcus pneumoniae* cell division? Environ Microbiol **15:** 3133-
740 3157.

741 Matsuzawa, H., Hayakawa, K., Sato, T., and Imahori, K. (1973) Characterization and genetic
742 analysis of a mutant of *Escherichia coli* K-12 with rounded morphology. J Bacteriol **115:**
743 436-442.

744 Meeske, A.J., Sham, L.T., Kimsey, H., Koo, B.M., Gross, C.A., Bernhardt, T.G., *et al*. (2015)
745 MurJ and a novel lipid II flippase are required for cell wall biogenesis in *Bacillus subtilis*.
746 Proc Natl Acad Sci USA **112:** 6437-6442.
747 Meeske, A.J., Riley, E.P., Robins, W.P., Uehara, T., Mekelanos, J.J., Kahne, D., *et al.* (2016)
748 SEDS proteins are a widespread family of bacterial cell wall polymerases. Nature
749 doi:10.1038/nature19331.
750 Mohammadi, T., van Dam, V., Sijbrandi, R., Vernet, T., Zapun, A., Bouhss, A., *et al*. (2011)
751 Identification of FtsW as a transporter of lipid-linked cell wall precursors across the
752 membrane. EMBO J **30:** 1425-1432.
753 Morlot, C., Zapun, A., Dideberg, O., and Vernet, T. (2003) Growth and division of *Streptococcus*
754 *pneumoniae*: localization of the high molecular weight penicillin-binding proteins during
755 the cell cycle. Mol Microbiol **50:** 845-855.
756 Morlot, C., Noirclerc-Savoye, M., Zapun, A., Dideberg, O., and Vernet, T. (2004) The D,D-
757 carboxypeptidase PBP3 organizes the division process of *Streptococcus pneumoniae*. Mol
758 Microbiol **51:** 1641-1648.
759 Noirclerc-Savoye, M., Lantez, V., Signor, L., Philippe, J., Vernet, T., and Zapun, A. (2013)
760 Reconstitution of membrane protein complexes involved in pneumococcal septal cell wall
761 assembly. PloS One **8:** e75522.
762 Nováková, L., Bezousková, S., Pompach, P., Spidlová, P., Sasková, L., Weiser, J., et al. (2010)
763 Identification of multiple substrates of the StkP Ser/Thr protein kinase in *Streptococcus*
764 *pneumoniae*. J Bacteriol **192:** 3629-3638.

765 Oliva, M.A., Halbedel, S., Freund, S.M., Dutow, P., Leonard, T.A., Veprintsev, D.B., et al. (2010)
766 Features critical for membrane binding revealed by DivIVA crystal structure. EMBO J **29:**
767 1988-2001.
768 Paik, J., Kern, I., Lurz, R., and Hakenbeck R. (1999) Mutational analysis of the *Streptococcus*
769 *pneumoniae* bimodular class A penicillin-binding proteins. J Bacteriol **181:** 3852-3856.
770 Pastoret, S., Fraipont, C., den Blaauwen, T., Wolf, B., Aarsman, M.E.G., Piette, A., *et al.* (2004)
771 Functional analysis of the cell division protein FtsW of *Escherichia coli*. J Bacteriol 186:
772 8370-8379.
773 Pereira, C.S., Thompson, J.A., and Xavier, K.B. (2013) AI-2-mediated signalling in bacteria.
774 FEMS Microbiol Rev **37:** 156-181.
775 Peters, K., Schweizer, I., Beilharz K., Stahlmann, C., Veening, J.W., Hakenbeck, R., *et al*. (2014)
776 *Streptococcus pneumoniae* PBP2x mid-cell localization requires the C-terminal PASTA
777 domains and is essential for cell shape maintenance. Mol Microbiol **92:** 733-755.
778 Philippe, J., Vernet, T., and Zapun, A. (2014) The elongation of ovococci. Microb Drug Resist
779 **20:** 215-221.
780 Rettner, R.E., and Saier Jr, M.H. (2010) The autoinducer-2 exporter superfamily. J Mol Microbiol
781 Biotechnol **18:** 195-205.
782 Ruiz, N. (2009) *Streptococcus pyogenes* YtgP (Spy_0390) complements *Escherichia coli* strains
783 depleted of the putitative peptidoglycan flippase MurJ. Antimicrob Agents Chemother **53:**
784 3604-3605.
785 Sauvage, E., Kerff, F., Terrak, M., Ayala, J.A., and Charlier, P. (2008) The penicillin-binding
786 proteins: structure and role in peptidoglycan biosynthesis. FEMS Microbiol Rev **32:** 234-
787 258.

788 Sham, L.T., Tsui, H.C.T., Land, A.D., Barendt, S.M., and Winkler, M.E. (2012) Recent advances
789 in pneumococcal peptidoglycan biosynthesis suggest new vaccine and antimicrobial
790 targets. Curr Opin Microbiol 15: 194-203.
791 Sham, L.T., Butler, E.K., Lebar, M.D., Kahne, D., Bernhardt, T.G., and Ruiz, N. (2014) MurJ is
792 the flippase of lipid-linked precursors for peptidoglycan biogenesis. Science **345:** 220-222.
793 Sibold, C., Henrichsen, J., König, A., Martin, C., Chalkley, L, and Hakenbeck, R. (1994) Mosaic
794 *pbpX* genes of major clones of penicillin-resistant *Streptococcus pneumoniae* have evolved
795 from *pbpX* genes of a penicillin-sensitive *Streptococcus oralis.* Mol Microbiol **12:** 1013-
796 1023.
797 Stewart, G.C. (2005) Taking shape: control of bacterial cell wall biosynthesis. Mol Microbiol **57:**
798 1177-1181.
799 Straume, D., Stamsås, G.A., and Håvarstein, L.S. (2015) Natural transformation and genome
800 evolution in *Streptococcus pneumoniae*. Infect Genet Evol **33:** 371-380.
801 Sun, X., Ge, F., Xiao, C.L., Yin, X.F., Ge, R., Zhang, L.H., et al. (2010) Phosphoproteomic
802 analysis reveals the multiple roles of phosphorylation in pathogenic bacterium
803 *Streptococcus pneumoniae*. J Proteome Res **9:** 275-282.
804 Sung, C.K., Li, H., Claverys, J.P., and Morrison, D.A. (2001) An *rpsL* cassette, Janus, for gene
805 replacement through negative selection in *Streptococcus pneumoniae*. Appl Environ
806 Microbiol **67:** 5190-5196.
807 Thibessard, A., Fernandez, A., Gintz, B., Leblond-Bourget, N., and Decaris, B. (2002) Effects of
808 *rodA* and *pbp2b* disruption on cell morphology and oxidative stress response of
809 *Streptococcus thermophilus* CNRZ368. J Bacteriol **184:** 2821-2826.

Tsui, H.C.T., Boersma, M.J., Vella; S.A., Kocaoglu, O., Kuru, E., Peceny, J.K., *et al.* (2014) Pbp2x localizes separately from Pbp2b and other peptidoglycan synthesis proteins during later stages of cell division of *Streptococcus pneumoniae* D39. Mol Microbiol **94:** 21-40.

Tsui, H.C.T., Zheng, J.J., Magallon, A.N., Ryan, J.D., Yunck, R., Rued, B.E., *et al.* (2016) Suppression of a deletion mutation in the gene encoding essential PBP2b reveals a new lytic transglycosylase involved in peripheral peptidoglycan synthesis in *Streptococcus pneumoniae* D39. Mol Microbiol doi: 10.1111/mmi.13366.

van den Ent, F., Amos, L.A., and Löwe, J. (2001) Prokaryotic origin of the actin cytoskeleton. Nature **413:** 39-44.

Vollmer, W. (2007) Preparation and analysis of pneumococcal murein (peptidoglycan). In Molecular biology of streptococci. Hakenbeck, R., and Chhatwal, S. (eds). Norfolk, United Kingdom: Horizon Bioscience, pp. 531-536.

Vollmer, W., Blanot, D., and de Pedro, M.A. (2008) Peptidoglycan structure and architecture. FEMS Microbiol Rev **32:** 149-167.

Wei, Y., Havasy, T., McPherson, D.C., and Popham, D.L. (2003) Rod shape determination by the *Bacillus subtilis* class B penicillin-binding proteins encoded by *pbpA* and *pbpH*. J Bacteriol **185:** 4717-4726.

Zapun, A., Vernet, T., and Pinho, M.G. (2008) The different shapes of cocci. FEMS Microbiol Rev **32:** 345-360.

833 **Table 1.** Strains used in this study.

Strain	Relevant characteristics	Source
R704	R6 derivative, Δ*comA*::*ermAM*; Ery^r	J. P. Claverys[a]
CP1500	Contains a novobiocin resistance gene, Nov^r	(Cato & Guild, 1968)
RH1	P704, but Δ*comA::ermAM, egb*::*spc*, Ery^R Spc^R	(Johnsborg *et al.*, 2008)
RH17	RH1 but Δ*cbpD*::Janus Spc^r, Ery^r, Kan^r	(Johnsborg *et al.*, 2008)
RH420	Δ*comM*::Janus, Spc^r, Cm^r Ery^r, Kan^r	(Eldholm *et al.*, 2009)
RH425	R704, but streptomycin resistant, Ery^r, Sm^r	(Johnsborg and Håvarstein, 2009)
SPH131	Δ*comA*, P1::P$_{comR}$::*comR*, P$_{comX}$::Janus, Ery^r, Kan^r	(Berg *et al.*, 2011)
SPH157	Δ*comA*, Δ*pbp2b*$_{wt}$, but expresses *pbp2b* ectopically from P$_{comX}$, Ery^r, Sm^r	(Berg *et al.*, 2013)
SPH164	Δ*comA*, Δ*pbp2x*$_{wt}$, but expresses *pbp2x* ectopically from P$_{comX}$, Ery^r, Sm^r	(Berg *et al.*, 2013)
SPH344	Δ*comA*, *ssbB*::*luc*, Δ*pbp1a*::Janus, Ery^r, Cm^r, Kan^r	This work
SPH345	Δ*comA*, *ssbB*::*luc*, Δ*pbp1b*::Janus, Ery^r, Cm^r, Kan^r	This work
SPH346	Δ*comA*, *ssbB*::*luc*, Δ*pbp2a*::Janus, Ery^r, Cm^r, Kan^r	This work
SPH347	Δ*comA*, Δ*egb*, *hirL*::*lacZ*, Δ*stkP*:Janus, Ery^r, Kan^r, Cm^r, Spc^r	This work
SPH348	Δ*comA*, Δ*mapZ*:Janus, Ery^r, Kan^r	This work
SPH349	Δ*comA*, Δ*pmp23*::Janus, Ery^r, Kan^r	This work
SPH350	Δ*comA*, Δ*mreC*, Ery^r, Sm^r	This work
SPH351	Δ*comA*, Δ*mreD*, Ery^r, Sm^r	This work
SPH352	Δ*comA*, Δ*rodZ*, Ery^r, Sm^r	This work
SPH353	Δ*comA*, Δ*gpsB*$_{wt}$, but expresses *gpsB* ectopically from P$_{comX}$, Ery^r, Sm^r, Spc^r	This work
SPH354	Δ*comA*, Δ*rodA*$_{wt}$, but expresses *rodA* ectopically from P$_{comX}$, Ery^r, Sm^r	This work
SPH355	Δ*comA*, Δ*spr0777*$_{wt}$, but expresses *spr0777* ectopically from P$_{comX}$, Ery^r, Sm^r	This work
SPH356	Δ*comA*, Δ*ftsB*$_{wt}$, but expresses *ftsB* ectopically from P$_{comX}$, Ery^r, Sm^r	This work
SPH357	Δ*comA*, Δ*ftsW*$_{wt}$, but expresses *ftsW* ectopically from P$_{comX}$, Ery^r, Sm^r	This work
SPH358	Δ*comA*, Δ*spr1357*$_{wt}$, but expresses *spr1357* ectopically from P$_{comX}$, Ery^r, Sm^r	This work
SPH359	Δ*comA*, Δ*murJ*$_{wt}$::Janus, but expresses *murJ* ectopically from P$_{comX}$, Ery^r, Sm^r	This work
SPH360	Δ*comA*, Δ*mltG*$_{wt}$, but expresses *mltG* ectopically from P$_{comX}$, Ery^r, Sm^r	This work
SPH361	Δ*comA*::*ermAM*, Δ*divIVA*::Janus, Ery^r, Kan^r	This work
SPH362	Native *divIVA* is replaced with *divIVA*$_{T201A}$, Ery^r, Sm^r	This work
SPH363	Native *divIVA* is replaced with *divIVA*$_{T201E}$, Ery^r, Sm^r	This work

SPH364	Native *divIVA* is replaced with *divIVAΔ40*, Ery^r, Sm^r	This work
SPH365	Native *divIVA* is replaced with *divIVAΔ65*, Ery^r, Sm^r	This work
SPH366	Native *divIVA* is replaced with *divIVAΔ74*, Ery^r, Sm^r	This work
SPH367	Native *divIVA* is replaced with *divIVAΔ92*, Ery^r, Sm^r	This work
SPH368	Native *divIVA* is replaced with *divIVAΔ112*, Ery^r, Sm^r	This work
SPH369	Native *divIVA* is replaced with *divIVA-GFP*, Ery^r, Sm^r	This work
SPH370	Native *divIVA* is replaced with *divIVAΔ92-GFP*, Ery^r, Sm^r	This work
SPH371	Native *divIVA* is replaced with *divIVAΔ112-GFP*, Ery^r, Sm^r	This work
SPH419	Δ*comA*, Δ*pbp2b*$_{wt}$, but expresses *pbp2b* ectopically from P$_{comX}$, Δ*cbpD::*Janus, Ery^r, Sm^r	This work
SPH420	Δ*comA*, Δ*mreD*, Δ*cbpD::*Janus, Ery^r, Sm^r	This work
SPH421	Δ*comA*::*ermAM*, Δ*divIVA*, Δ*cbpD*::Janus, Ery^r, Kan^r	This work
SPH422	Δ*comA*, Δ*rodA*$_{wt}$, but expresses *rodA* ectopically from P$_{comX}$, Δ*cbpD*::Janus Ery^r, Sm^r	This work
SPH423	Δ*comA*, Δ*spr0777*$_{wt}$, but expresses *spr0777* ectopically from P$_{comX}$, Δ*cbpD*::Janus Ery^r, Sm^r	This work

[a] Gift from Jean-Pierre Claverys.

844 **Table 2.** CbpD-susceptibility of strains in which proteins believed to be part of the divisome or

845 elongasome have been deleted or depleted.

Gene product	Function	Essential in R6	Deleted/ depleted	Susceptible to CbpD[1]
PBP1a	Glycosyltransferase/transpeptidase, peptidoglycan synthesis	No	Deleted	No
PBP2a	Glycosyltransferase/transpeptidase, peptidoglycan synthesis	No	Deleted	No
PBP1b	Glycosyltransferase/transpeptidase, peptidoglycan synthesis	No	Deleted	No
PBP2x	Transpeptidase, septal peptidoglycan synthesis	Yes	Depleted	No
PBP2b	Transpeptidase, lateral peptidoglycan synthesis	Yes	Depleted	Yes
MreC	Unknown role in lateral peptidoglycan synthesis	No	Deleted	No
MreD	Unknown role in lateral peptidoglycan synthesis	No	Deleted	Yes
GpsB	Unknown role in peptidoglycan synthesis	No	Depleted	No
DivIVA	Unknown role in peptidoglycan synthesis	No	Deleted	Yes
FtsW	Putative peptidoglycan polymerase, septal synthesis	Yes	Depleted	No
RodA	Peptidoglycan polymerase, lateral synthesis	Yes	Depleted	Yes
StkP	Serine/threonine kinase, involved in cell division	No	Deleted	No
MurJ	Putative lipid II flippase, peptidoglycan synthesis	Yes	Depleted	No
MltG	Putative endolytic transglycosylase, potential terminase	Yes	Depleted	No
MapZ	Early division site marker	No	Deleted	No
RodZ	Unknown role in lateral peptidoglycan synthesis	No[2]	Deleted	No
FtsB	Unknown role in septal peptidoglycan synthesis	Yes	Depleted	No
Pmp23	Peptidoglycan hydrolase	No	Deleted	No
Spr 0777	Unknown	Yes	Depleted	Yes
Spr 1357	Unknown	No	Depleted	No

846

847 [1]During competence, pneumococci synthesize and secrete the peptidoglycan hydrolase CbpD,
848 presumably to release donor-DNA from related strains and species sharing the same niche
849 (Straume *et al*., 2015). To protect themselves against CbpD, competent pneumococci express the
850 immunity protein, ComM, which is encoded by an early competence gene (Håvarstein *et al*., 2006).
851 All mutant strains in Table 1 are competent for natural transformation, and have a functional *comM*
852 immunity gene. Hence, they should be resistant to CbpD when secretion of this murein hydrolase
853 is induced by addition of CSP. However, despite having a functional *comM* gene, some
854 deletion/depletion mutants become highly susceptible to CbpD.

855 [2]Not essential in *S. pneumoniae* strain R6, but reported to be essential in *S. pneumoniae* strain D39
856 (Tsui *et al*., 2016).

857

858

859

860

Table 3. Phenotype of mutants harbouring various C-terminally truncated DivIVA proteins.

DivIVA[a]	C-terminal protein sequence[b]	Phenotype[c]	
		Long-chains	Immunity to CbpD
WT	-QRLKSTIESQLAIVESSDWEDILRPTATYLQTSDEAFKEVVSEVLGEPIPAPIEEEPIDM**T**R-QFSQAEMEELQARIEVADKELSEFEAQIKQEVETPTPVVSPQVEEEPLLIQLAQCMKNQK(262)	-	+
T201A	-QRLKSTIESQLAIVESSDWEDILRPTATYLQTSDEAFKEVVSEVLGEPIPAPIEEEPIDM**A**R-QFSQAEMEELQARIEVADKELSEFEAQIKQEVETPTPVVSPQVEEEPLLIQLAQCMKNQK(262)	-	+
T201E	-QRLKSTIESQLAIVESSDWEDILRPTATYLQTSDEAFKEVVSEVLGEPIPAPIEEEPIDM**E**R-QFSQAEMEELQARIEVADKELSEFEAQIKQEVETPTPVVSPQVEEEPLLIQLAQCMKNQK(262)	-	+
Δ40	-QRLKSTIESQLAIVESSDWEDILRPTATYLQTSDEAFKEVVSEVLGEPIPAPIEEEPIDM**T**R-QFSQAEMEELQARIEVADKE(222)	-	+
Δ65	-QRLKSTIESQLAIVESSDWEDILRPTATYLQTSDEAFKEVVSEVLGEPIPAPIEEEP(197)	-	+
Δ74	-QRLKSTIESQLAIVESSDWEDILRPTATYLQTSDEAFKEVVSEVLGEP(188)	-	+
Δ92	-QRLKSTIESQLAIVESSDWEDILRPTATYL(170)	+	+
Δ112	-QRLKSTIESQ(150)	+	-
ΔDivIVA		+	-

[a] Strains carrying various DivIVA mutations. WT= wild type strain. T201A and T201E indicate strains in which threonine at position 201 (underlined) in DivIVA has been substituted with alanine or glutamate. Δ40-Δ112 indicate the number of amino acids removed from the C-terminal end of DivIVA in mutant strains.

[b] The position of the last amino acids in WT and truncated DivIVA proteins is given at the end of the sequence. The underlined threonine (201) residue has been shown to be phosphorylated by StkP (Sun *et al*., 2010).

[c] DivIVA deletion mutants were tested for possible changes in morphology and immunity against the peptidoglycan hydrolase CbpD. Morphology: (-), cultures that mostly consist of diplococci and a small fraction of chains composed of 3-5 cells. (+), cultures consisting mostly of extremely long chains of cells (~50 >100 cells). Immunity to CbpD: (-), cultures that have lost immunity to CbpD and consequently lyse when induced to competence by the addition of CSP. (+), cultures that do not lyse when induced to competence.

Figure Legends

Fig. 1. DNA-release assay demonstrating CbpD-mediated autolysis in pneumococcal mutants during competence. Competent pneumococci express and secrete the peptidoglycan hydrolase CbpD, presumably to kill and lyse susceptible target cells and capture their DNA. To protect themselves against CbpD pneumococci express the ComM immunity protein, an integral membrane protein of unknown function. We discovered that pneumococcal strains deleted or depleted in PBP2b, MreD, RodA, DivIVA or Spr0777 are no longer immune to CbpD, despite having a functional *comM* gene. DNA release was measured in real time by culturing the cells in the presence of the membrane-impermeable Sytox Green Nucleic Acid Stain (Invitrogen™). Sytox Green fluoresces strongly upon binding DNA when excited at 485 nm. Competence was induced by addition of CSP (250 ng ml^{-1}) at the time points indicated by the arrows. Results were expressed as relative fluorescence units (RFU) and were normalized according to the number of cells at each time point. Solid lines; growth curves (OD_{492}) of wild type and mutant cultures. Dotted lines; relative fluorescence units (RFU) measured automatically every 5 min by a Synergy H1 Hybrid Reader. Panel (a), wild-type control (strain RH1); panel (b), strain RH420 (Δ*comM*); panel (c), strain SPH157 (depleted in PBP2b); panel (d), strain SPH351 (Δ*mreD*); panel (e), strain SPH361 (Δ*divIVA*); panel (f), strain SPH354 (depleted in RodA); and panel (g), strain SPH355 (depleted in Spr0777). Each experiment was repeated several times with similar results.

Fig. 2. Scanning electron microscopy images showing the long-chain phenotype characteristic of pneumococci in which PBP2b, DivIVA, MreD, RodA, and Spr0777 have been deleted or depleted.

903 Panel (a), strain RH425 (wild-type); panel (b), strain SPH350 (Δ*mreC*); panel (c), strain SPH361
904 (Δ*divIVA*); panel (d), strain SPH351 (Δ*mreD*); panel (e), strain SPH157 [ectopic expression of
905 PBP2b (grown in the presence of 0.02 µM ComS inducer)]; panel (f) strain SPH157 (depleted in
906 PBP2b); panel (g), strain SPH354 [ectopic expression of RodA (grown in the presence of 0.05 µM
907 ComS inducer); panel (h), strain SPH354 (depleted in RodA); panel (i), strain SPH355 [ectopic
908 expression of Spr0777 (grown in the presence of 0.2 µM ComS inducer)] and panel (j), strain
909 SPH355 (depleted in Spr0777). Different ComS concentrations were used for ectopic expression
910 of PBP2b, RodA and Spr0777. This was because different expression levels of these proteins are
911 required to give optimal growth of the respective mutant strain. Bars = 1µm.

912

913 **Fig. 3.** Removal of the C-terminal 112 amino acids of DivIVA causes mislocalization. Wild-type
914 DivIVA as well as the C-terminally truncated DivIVA mutants (DivIVA-Δ92 and DivIVA-Δ112)
915 were tagged with green fluorescent protein (GFP) at their C-terminal ends. The proteins were
916 expressed from the native P_{divIVA} promoter.

917

918 **Fig. 4.** Analysis of the stem peptide composition of peptidoglycan isolated from mutant strains
919 expressing different levels of PBP2b, DivIVA, MreD, RodA and Spr0777. A. HPLC profiles of
920 stem peptides after digesting purified peptidoglycan with LytA. PBP2b was expressed at high (2
921 µM ComS), intermediate (0.02 µM ComS) and low levels (depleted). RodA and Spr0777 were
922 expressed at low levels (depleted) and at levels that gave rise to normal cell morphology (see Fig.
923 2). For the sake of simplicity, we compared the amount of material eluting in peak I and II, the two
924 major peaks in the HPLC chromatogram. In a previous study (Berg *et al*., 2013), peak I and II

were analyzed by mass spectrometry, and found to consist of TetraTri and Tetra(SA)Tri peptides, respectively (see panel B). The ratio between peak I and peak II was used as a measure for the content of branched stem peptides in the peptidoglycan of the mutant strains under study. The stem peptide composition analyses were repeated two times with similar results.

Fig. 5. Interactions between the PBP2b, DivIVA, MreD, RodA and Spr0777 proteins detected by a bacterial two-hybrid approach. An *Escherichia coli* cya^- strain was co-transformed with plasmids containing the indicated fusions to adenylate cyclase fragments T18 and T25. Samples were spotted on agar plates containing X-gal and incubated for 24 hour at 30 ^{0}C. A blue colour indicates a positive interaction between the pair of fusion proteins tested, while a colourless spot indicates a negative result. Plasmids used for the positive and negative controls were supplied by Euromedex. The T25-PBP2b/Spr1357-T18 and T25-PBP2x/T18-RodA fusion pairs were included as examples of negative reactions.

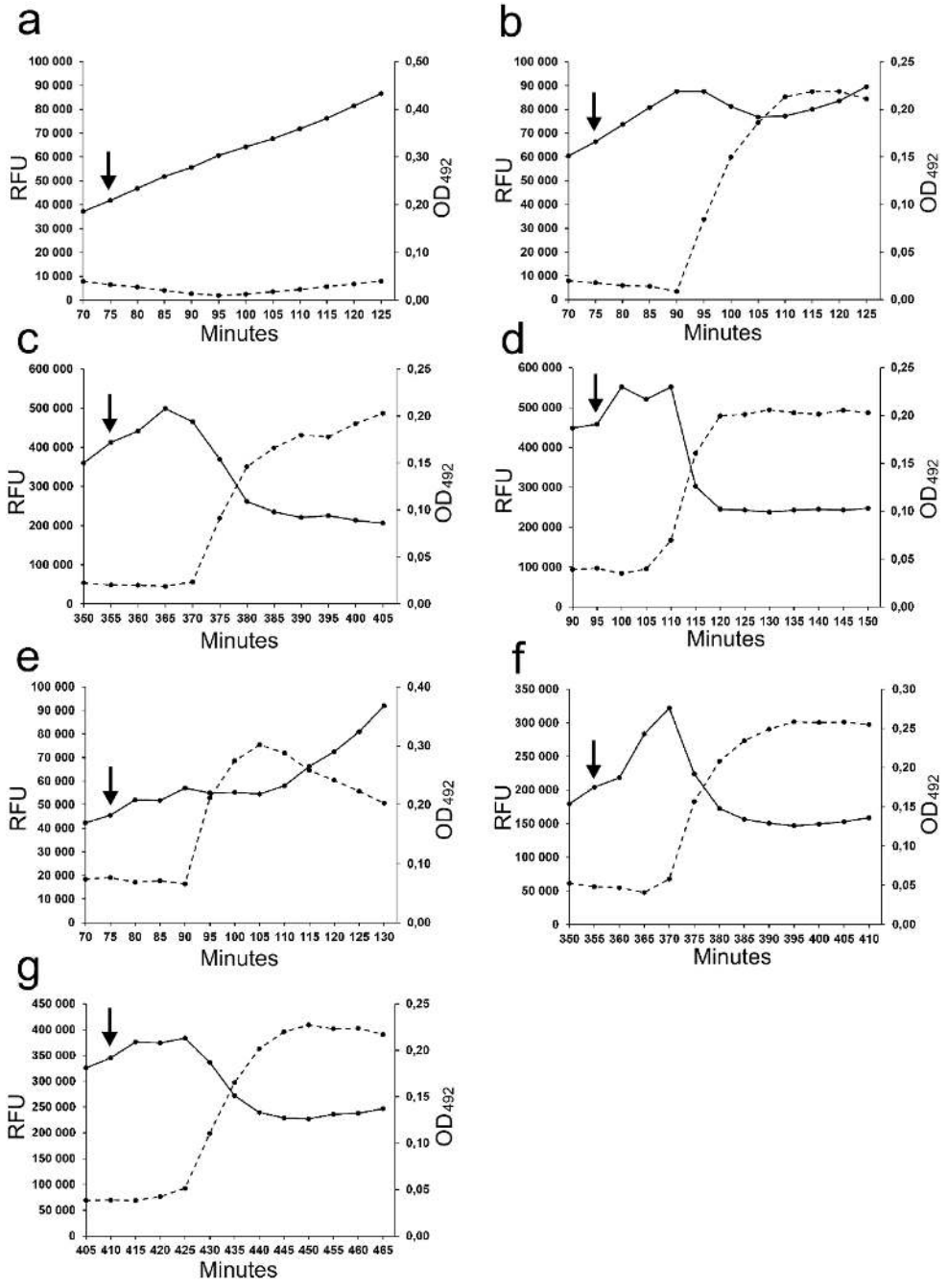

939

940 **Fig. 1.**

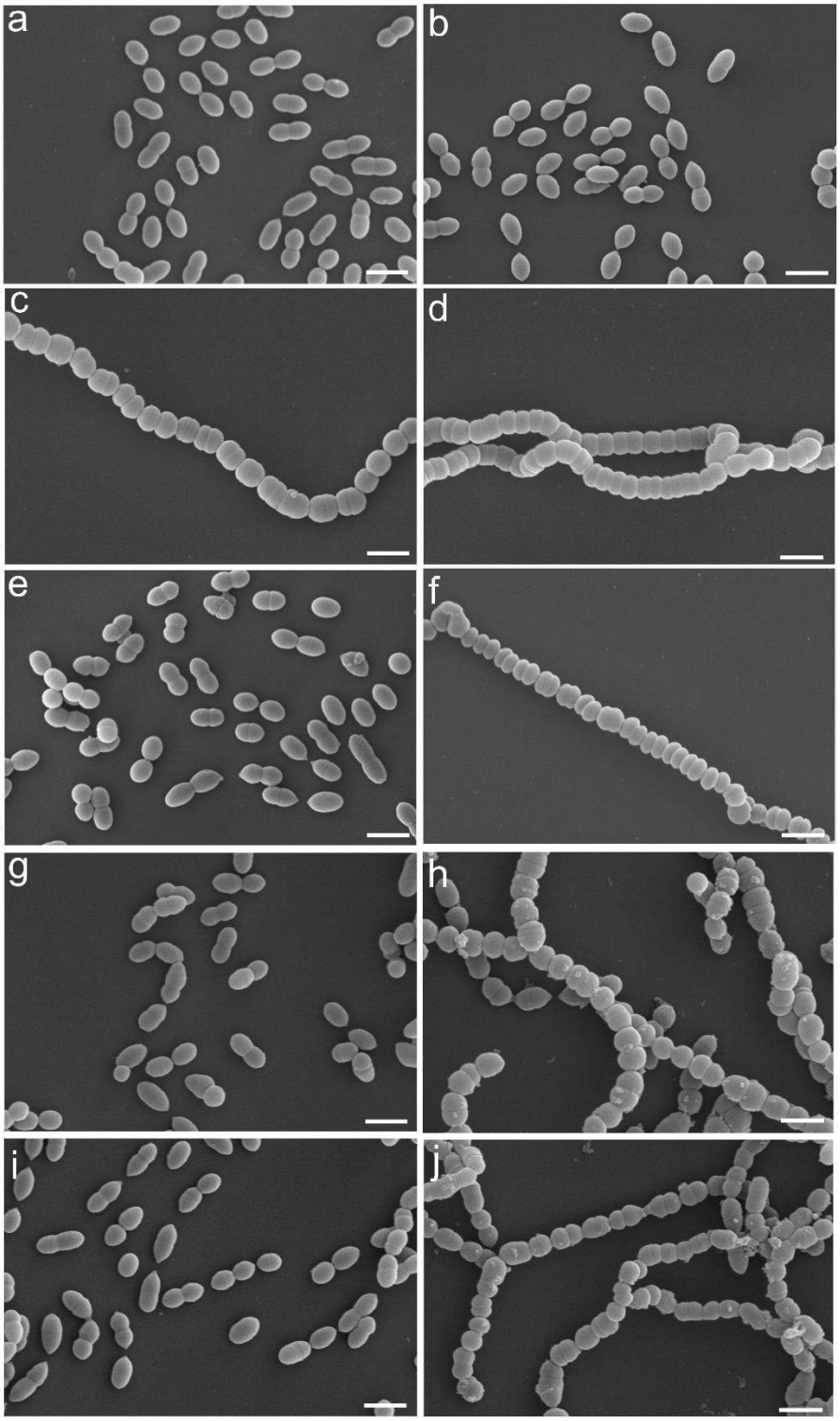

941

942 **Fig. 2.**

943

944

945

946

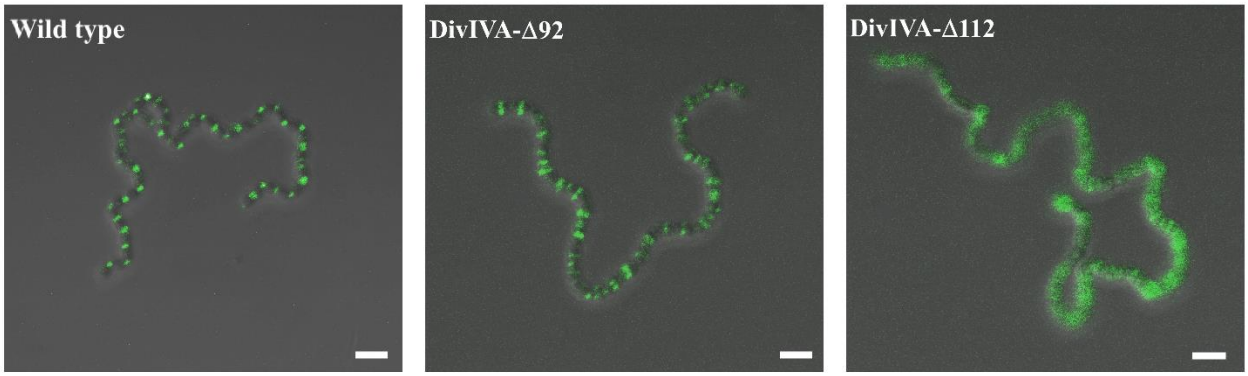

947

948 **Fig. 3.**

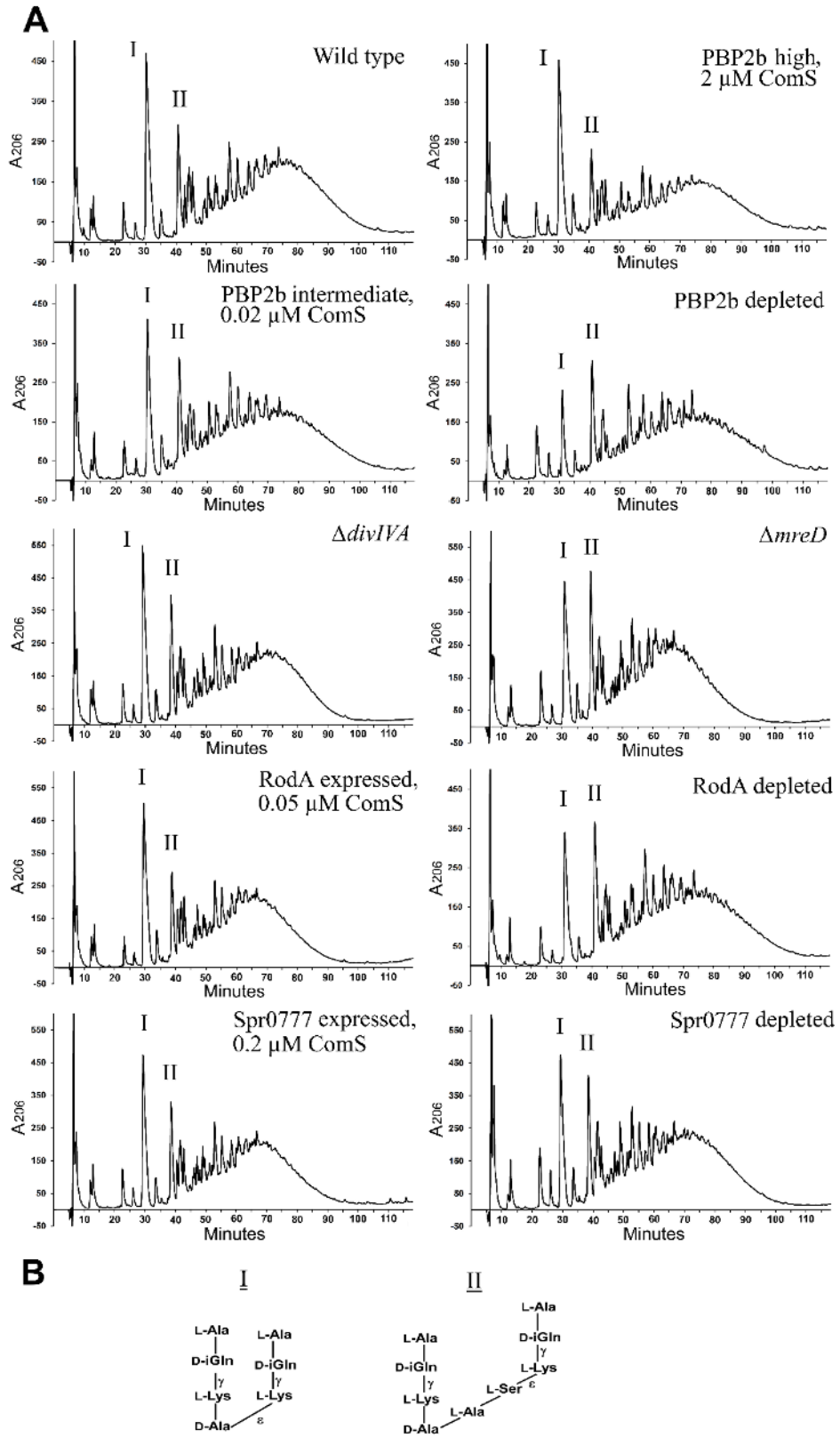
A
Wild type
PBP2b high, 2 µM ComS
PBP2b intermediate, 0.02 µM ComS
PBP2b depleted
ΔdivIVA
ΔmreD
RodA expressed, 0.05 µM ComS
RodA depleted
Spr0777 expressed, 0.2 µM ComS
Spr0777 depleted
I
II
A206
Minutes
B
I
II
L-Ala
D-iGln
L-Lys
D-Ala
L-Ser

949

950 **Fig. 4.**

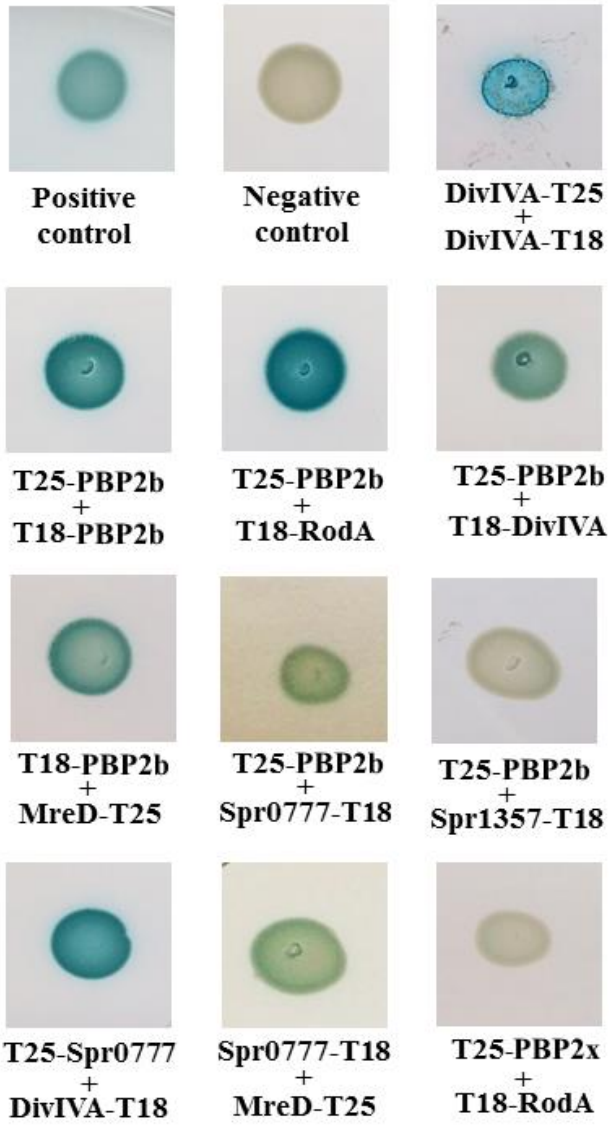
Positive control
Negative control
DivIVA-T25 + DivIVA-T18
T25-PBP2b + T18-PBP2b
T25-PBP2b + T18-RodA
T25-PBP2b + T18-DivIVA
T18-PBP2b + MreD-T25
T25-PBP2b + Spr0777-T18
T25-PBP2b + Spr1357-T18
T25-Spr0777 + DivIVA-T18
Spr0777-T18 + MreD-T25
T25-PBP2x + T18-RodA

Fig. 5

Graphical Abstract

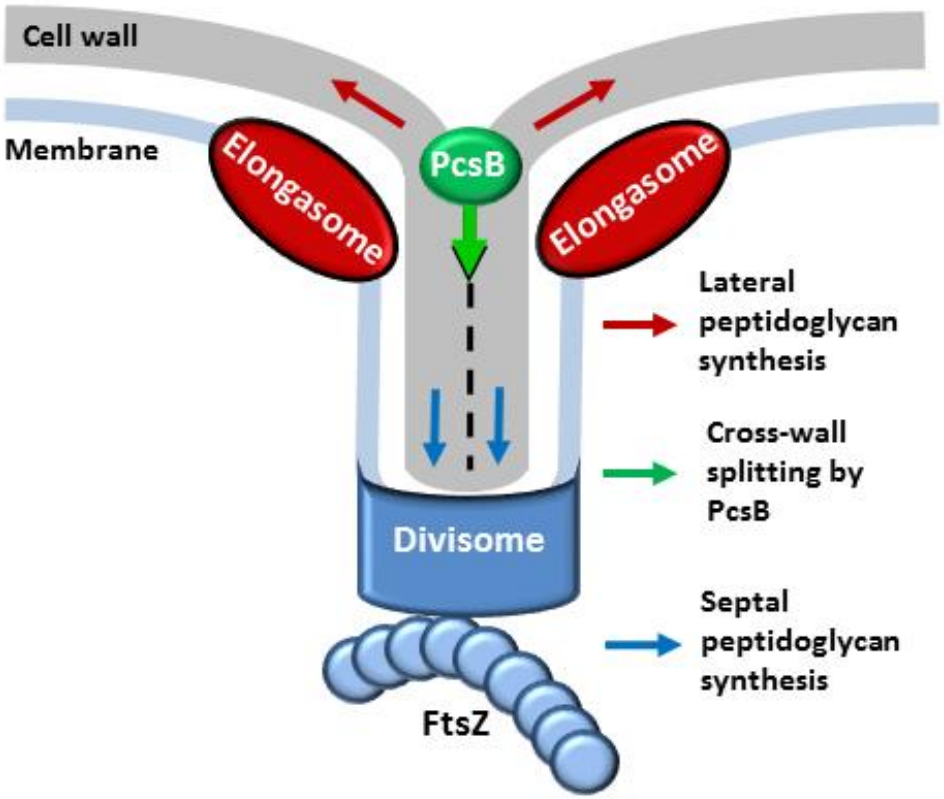

Supporting Information

Table S1. Oligonucleotide primer sequences

Name	Sequence (5'→ 3')	Reference
Primers used to amplify Janus		
Kan484.F	GTTTGATTTTTAATGGATAATGTG	(Johnsborg *et al.*, 2008)
RpsL41.R	CTTTCCTTATGCTTTTGGAC	(Johnsborg *et al.*, 2008)
khb94	AAGTATTTTCTAGTATTATAGCACATTTAACTTTCCTTATGCTTTTGGAC	This work
Primers used to amplify P_{comX} and the ΔP_{comX}::Janus amplicon		
khb31	ATAACAAATCCAGTAGCTTTGG	(Berg *et al.*, 2011)
khb33	TTTCTAATATGTAACTCTTCCCAAT	(Berg *et al.*, 2011)
khb34	CATCGGAACCTATACTCTTTTAG	(Berg *et al.*, 2011)
khb36	TGAACCTCCAATAATAAATATAAAT	(Berg *et al.*, 2011)
Primers used to create the Δ*cbpD* amplicon		
CbpD-1098	GTTGATTATCTTAGCAGCTCGT	Eldholm *et al.*, 2010)
CbpDR	CCAAGGGTTTGCTCGCAT	Eldholm *et al.*, 2010)
Primers used to create P_{comX}-*rodA* in a Δ*rodA* background		
ds339	ATTTATATTTATTATTGGAGGTTCAATGAAACGTTCTCTCGACTCTAG	This work
ds340	ATTGGGAAGAGTTACATATTAGAAATTATTTAATTTGTTTTAATACAACC	This work
ds342	AGAAAGTATTCGCTTTGAGTGC	This work
ds343	TCCAAAACCTGATCATTTCGATG	This work
css6	CACATTATCCATTAAAAATCAAACTACTATTTATCAAAGTTCATTAAAAAATC	This work
css7	TTAAATGTGCTATAATACTAGAAAATACTTGGAGAAAATCATGGTAAAAGTAG	This work
css15	CTACTTTTACCATGATTTTCTCCTACTATTTATCAAAGTTC	This work
css16	TAATGAACTTTGATAAATAGTAGGAGAAAATCATGGTAAAAGTAG	This work
Primers used to create P_{comX}-*ftsW* in a Δ*ftsW* background		
ds368	TCTCCTCAATTTCATAGAGTGTG	This work
ds369	ACAAGGCACGACGGTAAAGC	This work
css2	CACATTATCCATTAAAAATCAAACAGTATCACCACTCTACTAGG	This work
css3	TTAAATGTGCTATAATACTAGAAAATACTTGATAAAGAAAGGATAGTTTATGTC	This work
css9	TTTATATTTATTATTGGAGGTTCAATGAAGATTAGTAAGAGGCAC	This work
css10	GGGAAGAGTTACATATTAGAAACTACTTCAACAGAAGGTTCATTG	This work
css11	GACATAAACTATCCTTTCTTTATCAGTATCACCACTCTACTAGG	This work
css12	CCTAGTAGAGTGGTGATACTGATAAAGAAAGGATAGTTTATGTC	This work
Primers used to create the Δ*pbp2a* amplicon		
mts1.F	GCACAACTTGTTCGTACTCTTG	This work
mts2.R	CACATTATCCATTAAAAATCAAACGCGTTTATTTTATCATCTTCATC	This work
mts3.F	GTCCAAAAGCATAAGGAAAGGATGCTTGTCAAAGCCTAGC	This work

mts4.R	AGGTTTACTTCTGCAACTGTG	This work
Primers used to create the Δ*pbp1a* amplicon		
mts5.F	CCTTGTGTTCATAGCGAGG	This work
mts6.R	CACATTATCCATTAAAAATCAAACCTTGTTTTACCACCTAATAAATG	This work
mts7.F	GTCCAAAAGCATAAGGAAAGCATTTATCATCCAGATTTTTCTG	This work
mts8.R	AAAACGGCTTTGGTAGCAGATG	This work
Primers used to create the Δ*pbp1b* amplicon		
mts9.F	GCCTGTACTTGGTAGTTTGG	This work
mts10.R	CATTATCCATTAAAAATCAAACGGATTTCCTCACTTTATCTATTA	This work
mts11.F	GTCCAAAAGCATAAGGAAAGTTCTCTAAATGAAGTGGCCAATC	This work
mts12.R	GACTATTCCAGTATAGCAC	This work
Primers used to create the Δ*stkP* amplicon		
khb410	AGAAATATTAGGTAGTGTTTGTC	This work
khb411	CCAGACAGTCATGCCCAAAATC	This work
gs321	AATTGCACATCTCAAATAACTACTCATTCTGCATCCTCCTCGT	This work
gs322	CGTCCAAAAGCATAAGGAAAGAAGCAGATGGATAATCAAAATGA	This work
Primers used to create the Δ*mapZ* amplicon		
ds239	TGCAGAAACACTATGCTCGC	This work
ds240	CACATTATCCATTAAAAATCAAACGAGTATCCCTTTCTATTTTACC	This work
ds241	GTCCAAAAGCATAAGGAAAGGCAGTCGTTACAAAATTCTTTC	This work
ds242	TACCAGTTCCCTTGTTACCTG	This work
Primers used to create the Δ*pmp23* amplicon		
ds301	ATGATACCGAGCTGTTCTTAG	This work
ds302	CACATTATCCATTAAAAATCAAACTTATTTACTTTGGATATCCTCGA	This work
ds303	GTCCAAAAGCATAAGGAAAGACCAGGTGTTTTTGTTATAAGTTTTC	This work
ds304	AAGGTTTTAGTGAAATCTGCATTG	This work
Primers used to create the P$_{comX}$-*mreC* and Δ*mreC* amplicons		
gs223	ATGGATAGTATGATTTTGGGG	This work
gs224	CTACGAGCTTGTTTTTCCAAC	This work
gs225	CACATTATCCATTAAAAATCAAACATCCCTACCTTTATATCAAAAAC	This work
gs226	AAATACTTGTGGAGGTTCCATTAATTAGTGGGGAATTCATAATG	This work
gs227	ATTTATATTTATTATTCGAGGTTCAATGAACCGTTTTAAAAAATCAAAAT	This work
gs228	ATTGGGAAGAGTTACATATTAGAAATTATGAATTCCCCACTAATTCTA	This work
gs229	ATCCCTACCTTTATATCAAAAAC	This work
gs230	GTTTTTGATATAAAGGTAGGGATAATTAGTGGGGAATTCATAATG	This work
Primers used to create the P$_{comX}$-*mreD* and Δ*mreD* amplicons		
gs231	GTCAATACCGACAATTGAAATG	This work
gs232	ACGGACAGGTGCTGCTGC	This work
gs233	CACATTATCCATTAAAAATCAAACTTATGAATTCCCCACTAATTCTA	This work
gs234	CGTCCAAAAGCATAAGGAAAGGAACGACATATAAATGTAACAAA	This work
gs235	TTATGAATTCCCCACTAATTCTA	This work
gs236	TAGAATTAGTGGGGAATTCATAAGAACGACATATAAATGTAACAAA	This work

gs237	ATTTATATTTATTATTCGAGGTTCAATGAGACAGTTGAAGCGAGTT	This work
gs238	ATTGGGAAGAGTTACATATTAGAAATTATAGATAATATTTTTCAAAAATAAAT	This work
Primers used to create the Δ*rodZ* amplicon		
khb445	TAGATTTACTTGATGAATTGGTAA	This work
khb446	CACATTATCCATTAAAAATCAAACACTTGTCATCCCTTCTTTCTAG	This work
khb447	TTAAATGTGCTATAATACTAGAAAATACTTGTGGAGGTTCCATTGGAAAAACGAATGAAAAAAGAAC	This work
khb448	CCACACGTTGCTTTTGGCC	This work
Primers used to create the Δ*gpsB* amplicon		
gs301	CATCGGAATCGCACGTTTTTG	This work
gs302	CGTTTAAAGAGGCTAGACCC	This work
khb413	ATTTATATTTATTATTGGAGGTTCAATGGAGAGAGACATGGCAAG	This work
khb414	ATTGGGAAGAGTTACATATTAGAAATTAAAAATCTGAGTTATCTAAAATTT	This work
khb415	TTTAAATAACAGATTAAAAAAATTATAAGTAGTTATTTGAGATGTGCAATT	This work
khb416	GTATTCAAATATATCCTCCTCACTCTCGCTTGCTAGTATTATTATA	This work
Primers used to create P$_{comX}$-*spr0777* in a Δ*spr0777* background		
khb480	ATTTATATTTATTATTGGAGGTTCAATGTTTCGTAGAAATAAATTATTTTTT	This work
khb481	ATTGGGAAGAGTTACATATTAGAAATTACTTAGCTAATTCTCTTTCTC	This work
khb482	ACGATTTTGCGAAGTGTAAATG	This work
khb483	CACATTATCCATTAAAAATCAAACGAGTTACCTCCCTCACTTTAT	This work
khb484	GTCCAAAAGCATAAGGAAAGAAGTCAGGAGAACCCTGATTT	This work
khb485	AAGGAATAATGGAGCCGGTG	This work
Primers used to create P$_{comX}$-*ftsB* in a Δ*ftsB* background		
ds293	ATTTACAAGAAAATTCGTCAAATTG	This work
ds294	CACATTATCCATTAAAAATCAAACTTAGACATTTTCTTCTACCCGTG	This work
ds295	GTCCAAAAGCATAAGGAAAGTAAAATGGAAAATTTATTAGACGTA	This work
ds296	CAGTCGTATCTAACTGATAAAG	This work
ds297	TACGTCTAATAAATTTTCCATTTTATTAGACATTTTCTTCTACCCGTG	This work
ds298	CACGGGTAGAAGAAAATGTCTAATAAAATGGAAAATTTATTAGACGTA	This work
ds299	ATTTATATTTATTATTGGAGGTTCAATGTCTAAAAATATTGTACAATTGA	This work
ds300	ATTGGGAAGAGTTACATATTAGAAATCACCTTTGAAGCAAGTCAGG	This work
Primers used to create P$_{comX}$-*murJ* in a Δ*murJ* background		
khb392	GTTGAAGTTGCCAATGAGTTG	This work
khb393	CACATTATCCATTAAAAATCAAACAGATTCCTCATTCAATTTTGATAA	This work
khb394	GTCCAAAAGCATAAGGAAAGGGTAGCATTTATAAATAAAAGGAA	This work
khb395	TTACGTTCCAGTGATTCTTGG	This work
khb396	ATTTATATTTATTATTGGAGGTTCAATGTCGCACGAAAACAATCAC	This work
khb397	ATTGGGAAGAGTTACATATTAGAAATTACGAAAGCTTAAATTTTGCTC	This work
Primers used to create P$_{comX}$-*mltG* in a Δ*mltG* background		

ds355	CACATTATCCATTAAAAATCAAACAAGTTTTTCCTCCTTGTTGATAA	This work
ds356	GTGCTATAATACTAGAAAATACTTACAAACTAAAATTATGTGATACTTC	This work
ds357	AAGTTTTTCCTCCTTGTTGATAA	This work
ds358	TTATCAACAAGGAGGAAAAACTTACAAACTAAAATTATGTGATACTTC	This work
ds359	ATTTATATTTATTATTGGAGGTTCATTGAGTGAAAAGTCAAGAGAAG	This work
ds360	ATTGGGAAGAGTTACATATTAGAAATTAGTTTAATTTGCTGTTGACATG	This work
ds361	AAACTAGCCGCAGGTTGCTC	This work
ds362	AATTAAGATCATTCAGGCAAGC	This work
Primers used to create P_{comX}-*spr1357* in a Δ*spr1357* background		
khb496	ATTTATATTTATTATTGGAGGTTCAATGGAGCAAAAAGAGAAACATTT	This work
khb497	ATTGGGAAGAGTTACATATTAGAAACTATTGTTCACTCTTGACTTCC	This work
khb498	TCACGTGGAGTCTGACCATG	This work
khb499	CACATTATCCATTAAAAATCAAACAAATACTTCCTTTCTATTGTTCTC	This work
khb500	GTCCAAAAGCATAAGGAAAGGTAGTCAGTGGTCTATATGAAT	This work
khb501	CTGGCTCCTCACTCTGCAA	This work
Primers used to create the Δ*divIVA* amplicon		
gs287	CCTGATTTTGGTAGCCTTCG	This work
gs288	CATAGTAAAGGGAAGTTGAAAC	This work
gs289	CACATTATCCATTAAAAATCAAACTCACTTACTTAATAATAACTGGAC	This work
gs290	CGTCCAAAAGCATAAGGAAAGCTCCAGTGCATCCGACAGG	This work
Primers used to create the *divIVA*$_{T201A}$ amplicon		
ds204	GCACGTCAGTTCTCTCAAGCAG	This work
ds205	CTGCTTGAGAGAACTGACGTGCCATATCAATTGGTTCTTCTTCAA	This work
Primers used to create the *divIVA*$_{T201E}$ amplicon		
ds208	GAACGTCAGTTCTCTCAAGCAG	This work
ds209	CTGCTTGAGAGAACTGACGTTCCATATCAATTGGTTCTTCTTCAA	This work
Primers used to create the *divIVAΔ40, divIVAΔ65, divIVAΔ74, divIVAΔ92 and divIVAΔ112* amplicons		
dS226	CCTGTCGGATGCACTGGAGTTATTCTTTATCGGCTACCTCAATAC	This work
dS227	CCTGTCGGATGCACTGGAGTTATGGTTCTTCTTCAATTGGAGC	This work
dS245	CCTGTCGGATGCACTGGAGTTACGGTTCTCCAAGTACTTCG	This work
dS246	CCTGTCGGATGCACTGGAGTTAAAGATAAGTAGCTGTTGGACG	This work
dS247	CCTGTCGGATGCACTGGAGTTACTGACTCTCAATTGTAGATTTG	This work
Primers used to create the *divIVA-GFP, divIVAΔ92-GFP and divIVAΔ112-GFP* amplicons		
ds210	CTCTAGACTTCTGGTTCTTCATCTTCTGGTTCTTCATACATTG	This work
ds211	ATGAAGAACCAGAAGTCTAGAGGATCTGGTGGAGAAGCTGCAGCTAAAGCTGGAACTAGTATCAAACATCTTACCGGTTCTAAAGG	This work
ds212	CCTGTCGGATGCACTGGAGTTATGCGGCCGCTCCACTAG	This work
ds366	CTCTAGACTTCTGGTTCTTCATAAGATAAGTAGCTGTTGGAC	This work
ds367	CTCTAGACTTCTGGTTCTTCATCTGACTCTCAATTGTAGATTTG	This work
Primers used to create T25 and T18 fusions of *pbp2b*, *mreD*, *divIVA*, *spr0777*, *rodA*, *pbp2x* and *spr1357* (restriction sites are underlined)		
KHB426 Fwd *pbp2b*	TACGGGATCCCAGAAAATTTAACAGCCATTCGAT	This work

KHB427 Rev *pbp2b*	TACGGAATTCCTAATTCATTGGATGGTATTTTTG	This work
KHB428 Fwd *divIVA*	TACGAAGCTTGGTGAGGAATAGAATGCCAATT	This work
KHB453 Fwd *divIVA*	TACGGGATCCCAGGAATAGAATGCCAATTACATC	This work
KHB454 Rev *divIVA*	TACGGAATTCCTACTTCTGGTTCTTCATACAT	This work
GS.334 Rev *divIVA*	TACGGAATTCGACTTCTGGTTCTTCATACATTGG	This work
KHB462 Rev *rodA*	TACGGAATTCTTATTTAATTTGTTTTAATACAACCT	This work
DS341 Fwd *rodA*	TACGGGATCCCAAACGTTCTCTCGACTCTAGAG	This work
KHB486 Fwd *pbp2x*	TACGTCTAGAG AAGTGGACAAAAAGAGTAATCC	This work
KHB487 Rev *pbp2x*	TACGGAATTCTTAGTCTCCTAAAGTTAATGTAAT	This work
KHB505 Rev *spr1357*	TACGTGAATTCGATTGTTCACTCTTGACTTCCTC	This work
KHB506 Fwd *srp1357*	TACGACTCTAGAGATGGAGCAAAAAGAGAAACATTT	This work
GS.337 Fwd *spr0777*	GATCGGATCCCATGTTTCGTAGAAATAAATTATTTTT	This work
GS.338 Rev *spr0777*	GATCGAATTCGACTTAGCTAATTCTCTTTCTCGT	This work
GS.339 Rev *spr0777*	GATCGAATTCTTACTTAGCTAATTCTCTTTCTC	This work
DS345 Fwd *mreD*	TACGTCTAGAGATGAGACAGTTGAAGCGAGTTG	This work
DS350 Rev *mreD*	TACGGAATTCGAGGTTCCTCCTCCTCCACTTCCTCCTCCT CCTAGATAATATTTTTCAAAAATAAATTG	This work

Berg, K.H., Biørnstad, T.J., Straume, D., and Håvarstein, L.S. (2011) Peptide-regulated gene depletion system developed for use in *Streptococcus pneumoniae*. J Bacteriol **193**: 5207-5215.

Eldholm, V., Johnsborg, O., Straume, D., Solheim Ohnstad, H., Berg, K.H., Hermoso, J.A., Håvarstein, L.S. (2010) Pneumococcal CbpD is a murein hydrolase that requires a dual cell envelope binding specificity to kill target cells during fratricide. Mol Microbiol **76**: 905-917

Johnsborg, O., Eldholm, V., Bjørnstad, M.L., and Håvarstein, L.S. (2008) A predatory mechanism dramatically increases the efficiency of lateral gene transfer in *Streptococcus pneumoniae* and related commensal species. Mol Microbiol **69:** 245-253.

997

998 **Table S2.** The peak area ratio between peak I and peak II in Fig. 4.

999

Strain	Gene deleted	Gene ectopically expressed	ComS[1] inducer (μM)	Peak I/Peak II		
				Exp. 1	Exp. 2	Average
RH1[2]	NA[3]	NA	NA	2.7	2.4	2.6
SPH157	NA	*pbp2b*	2	3.3	3.1	3.2
SPH157	NA	*pbp2b*	0.02	2.1	2.2	2.2
SPH157	NA	*pbp2b*	0	0.8	0.8	0.8
SPH351	*mreD*	NA	NA	1.7	1.6	1.7
SPH354	NA	*rodA*	0.05	3.1	3.2	3.2
SPH354	NA	*rodA*	0	1.2	1.2	1.2
SPH355	NA	*spr0777*	0.2	2.2	2.1	2.2
SPH355	NA	*spr0777*	0	1.7	1.7	1.7
SPH361	*divIVA*	NA	NA	2.2	2.1	2.2

1000 [1] Depletion of target genes was performed by removing ComS from the medium (0 μM ComS).
1001 A ComS concentration of 2 μM induces the maximum rate of transcription from the P_{comX}
1002 promoter. ComS concentrations of 0.02, 0.05 and 0.2 μM was found to give wild-type-like
1003 morphologies and growth rates in the SPH157, SPH354 and SPH355 strains, respectively. [2]Wild-
1004 type strain. [3]Non applicable.

1005

1006

1007

1008

1009

1010

1011

1012

1013

1014

1015

1016

1017

1018

Table S3. Plasmids used for BACTH analysis

Plasmids	Relevant characteristics	Reference
pKT25	For fusing the T25 domain at the N-terminus, Kan^R.	Euromedex
pKNT25	For fusing the T25 domain at the C-terminus, Kan^R.	Euromedex
pUT18C	For fusing the T18 domain at the N-terminus, Amp^R.	Euromedex
pUT18	For fusing the T18 domain at the C-terminus, Amp^R.	Euromedex
pKT25-zip	Expresses T25 fused to a leucine zipper domain, Kan^R.	Euromedex
pUT18C-zip	Expresses T18 fused to a leucine zipper domain, Amp^R.	Euromedex
pKT25-pbp2b	Expresses Pbp2b with the T25 domain fused at its N-terminus, Kan^R.	This work
pUT18C-pbp2b	Expresses Pbp2b with the T18 domain fused at its N-terminus, Amp^R.	This work
pKT25-pbp2x	Expresses Pbp2x with the T25 domain fused at its N-terminus, Kan^R.	This work
pUT18C-rodA	Expresses RodA with the T18 domain fused at its N-terminus, Amp^R.	This work
pUT18C-divIVA	Expresses DivIVA with the T18 domain fused at its N-terminus, Amp^R.	This work
pUT18-divIVA	Expresses DivIVA with the T18 domain fused at its C-terminus, Amp^R.	This work
pKNT25-divIVA	Expresses DivIVA with the T25 domain fused at its C-terminus, Kan^R.	This work
pKT25-spr0777	Expresses Spr0777 with the T25 domain fused at its N-terminus, Kan^R.	This work
pUT18-spr0777	Expresses Spr0777 with the T18 domain fused at its C-terminus, Amp^R.	This work
pKNT25-mreD	Expresses MreD with the T25 domain fused at its C-terminus, Kan^R.	This work
pUT18-spr1357	Expresses Spr1357 with the T25 domain fused at its C-terminus, Amp^R.	This work

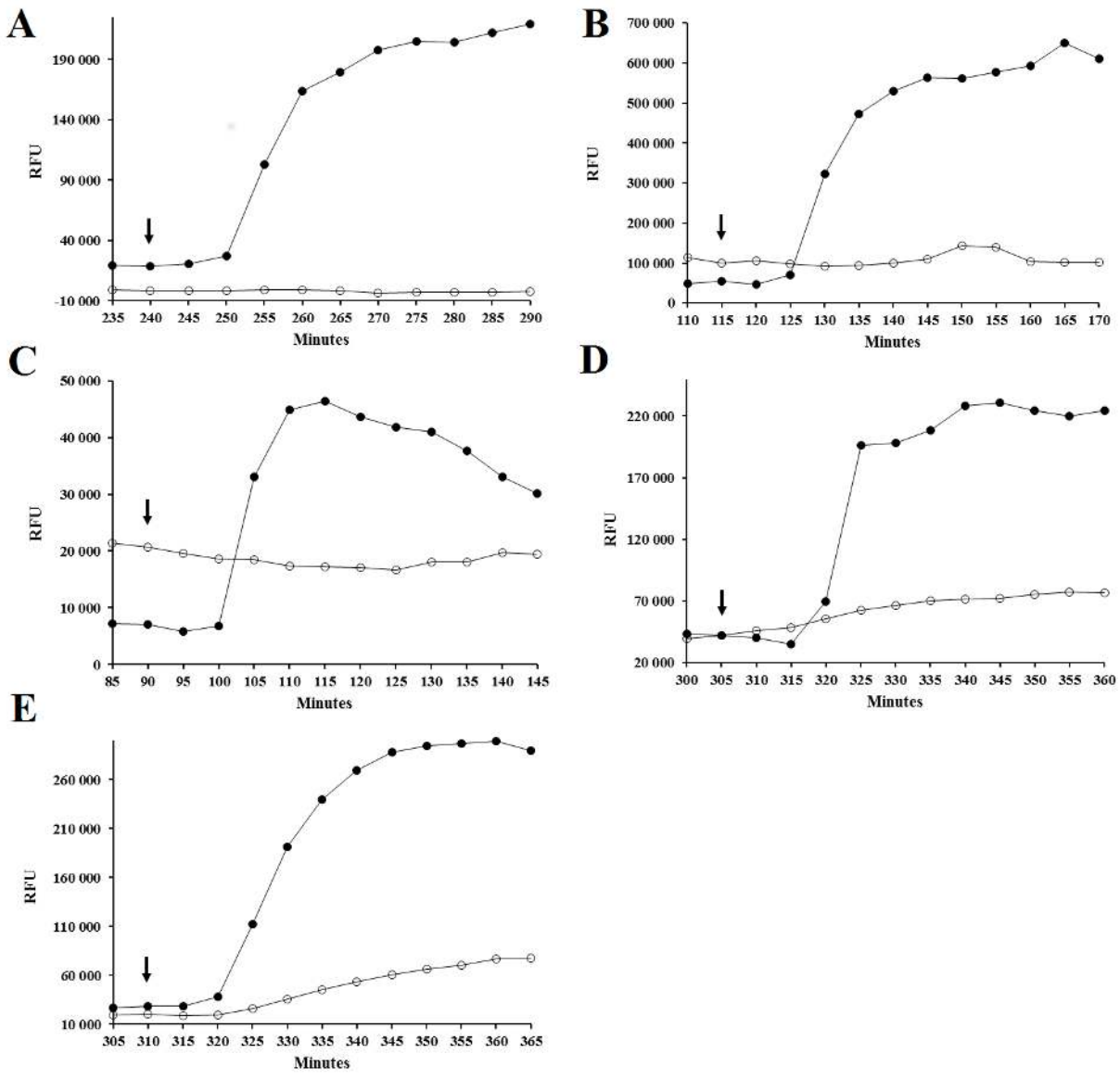

Fig. S1. DNA-release assay demonstrating that competence induced autolysis in pneumococcal mutants deleted or depleted in PBP2b, MreD, RodA, DivIVA or Spr0777 is caused by CbpD. DNA release was measured in real time by culturing the cells in the presence of the membrane-impermeable Sytox Green Nucleic Acid Stain (Invitrogen™). Sytox Green fluoresces strongly upon binding DNA when excited at 485 nm. Competence was induced by addition of CSP (250 ng ml^{-1}) at the time points indicated by the arrows. The fluorescence was measured automatically

every 5 min by a Synergy H1 Hybrid Reader. Results were expressed as relative fluorescence units (RFU) and were normalized according to the number of cells at each time point. Solid lines; *cbpD*$^{+}$ cultures. Dotted lines; Δ*cbpD* cultures. Panel (a), strains SPH157^{CbpD+} and SPH419$^{\Delta cbpD}$ (both depleted in PBP2b); panel (b), strains SPH351^{CbpD+} and SPH420$^{\Delta cbpD}$ (both Δ*mreD*); panel (c), strains SPH361^{CbpD+} and SPH421$^{\Delta cbpD}$ (both Δ*divIVA*); panel (d), strains SPH354^{CbpD+} and SPH422$^{\Delta cbpD}$ (both depleted in RodA); panel (e), strains SPH355^{CbpD+} and SPH423$^{\Delta cbpD}$ (both depleted in Spr0777).